Chapter 9

The Characterization of Small-Sized Obsidian Debitage Using P-XRF: A Case Study from Arequipa, Peru

David A. Reid
University of Illinois at Chicago

Patrick Ryan Williams
Field Museum of Natural History and the University of Illinois at Chicago

Kurt Rademaker
Michigan State University

Nicholas Tripcevich
University of California Berkeley

Michael D. Glascock
University of Missouri

Abstract

The use of portable-XRF has allowed for greater ease of obsidian characterization worldwide, as the technique is relatively fast, inexpensive, and non-destructive. This has proven ideal for the analysis of obsidian artifacts within museum collections and archaeological field materials. Comprehensive analyses of large obsidian assemblages, including small-sized debitage, has increasingly identified rare, exotic obsidian sources not commonly found within archaeological contexts. However, due to the analytical limitations of pXRF, factors of specimen size, thickness, and surface irregularity create challenges for the accurate characterization of small obsidian fragments. In this chapter we report the efforts taken by The Field Museum's Elemental Analysis Facility in the characterization of obsidian artifacts from the Majes Valley of Arequipa, Peru dating to the Middle Horizon period (AD 600–1000). Approaches include direct comparison of artifact geochemical data to Andean geologic reference materials alongside several multivariate analyses to mitigate issues of specimen size. Our conclusions show the reliability of pXRF for the characterization of small obsidian debitage and its significance as it allowed us to reconstruct previously unknown caravan routes linking the Majes Valley to interior highland zones.

Introduction

The application of portable-XRF (pXRF) has allowed for wider accessibility and analysis of obsidian artifacts worldwide, as it is a rapid, non-destructive, and relatively inexpensive technique. This is especially true for Andean obsidian provenance studies conducted in museum and field settings over the last two decades (Bélisle *et al.* 2020; Craig *et al.* 2007; Giesso *et al.* 2020; Kellett *et al.* 2013; Matsumoto *et al.* 2018; Williams *et al.* 2012). Portable handheld XRF instruments allow the researcher to analyze an entire obsidian assemblage from formal tools down to small debitage (i.e. the waste product of lithic tool production). This is especially pertinent as restrictions on the export of lithic tools and/or their destruction during geochemical analysis is commonplace. However, various analytical limitations and challenges are present in the use of pXRF. These include issues of precision, or the "repeatability and stability of measurement" and accuracy, or how measurements conform to "correct" values (Hughes 1998: 108; see also Frahm 2013; Nazaroff *et al.* 2010; Speakman and Shackley 2013).

As a result of comprehensive analyses of total obsidian assemblages through pXRF, archaeologists have a greater likelihood of encountering small, rare obsidian sources not commonly identified that may only comprise < 1% of the overall artifact assemblage (e.g., Bélisle *et al.* 2020). Obsidian attributes related to material quality, abundance, and distance to the source are key factors in lithic production and the geologic

[1] Contact author: David A. Reid, Department of Anthropology, University of Illinois at Chicago, 1007 West Jackson Street, 2102 BSB Chicago, IL 60607. dreid5@uic.edu

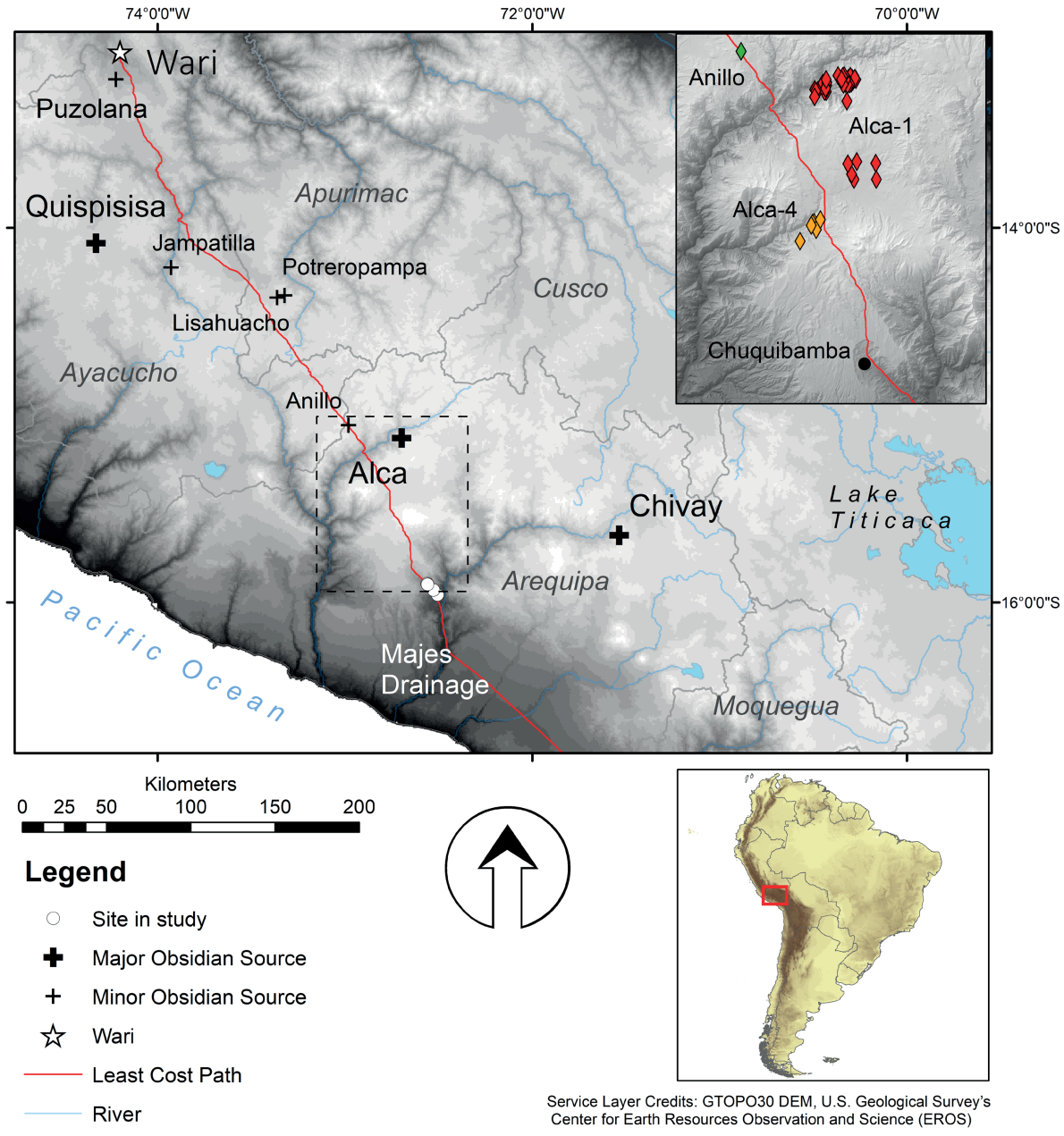

Figure 9.1. Base map of south-central Peru showing major and minor obsidian sources and the study region.

provenance of lithic types (Andrefsky 1994). Following Eerkens *et al.* (2007), the provenance of formal tools and small flake debitage, produced from periodic tool maintenance, may best indicate source diversity and transport distance.

Complete flaked stone tools are not always archaeologically deposited in the same area as their production or maintenance. Thus, debitage analyses are critical to reconstruct prehistoric lithic use and the entire operational chain from lithic source exploitation to finished tool (Andrefsky 2007; Sullivan and Rozen 1985). This makes the geochemical characterization of small obsidian flakes an ideal material to trace long-distance regional interactions and patterns of exchange, especially those related to tool curation and late-stage production. However, accurate pXRF analysis of small obsidian debitage is greatly impacted by issues of specimen size, thickness, and surface irregularity (Davis *et al.* 2011), making conclusive identifications of rare sources especially problematic.

In this chapter, we present results of a pXRF analysis of 303 obsidian artifacts recovered from four archaeological sites located in the Department of Arequipa in southern Peru. Nearly 80% of this assemblage corresponds to

debitage including specimens that would normally be overlooked or left unanalyzed by pXRF due to their small size. Here we document the specific methodological approach taken to characterize these materials including multivariate analyses (following Glascock 1998 and Frahm 2016) and comparisons to Andean geologic obsidians analyzed with the same instrument and settings. Our results demonstrate the utility of pXRF in the accurate characterization of small-sized obsidian debitage and its broader significance to reconstructing prehistoric obsidian use and exchange. In comparison to formal tools, small-sized obsidian debitage show a greater diversity in geologic source and maximum distance from the study area. Using GIS cost-path analysis and regional studies of prehistoric roads, we also show how small-sized debitage allows us to reconstruct previously unknown caravan routes between Peru's montane valleys and interior highland zones.

Samples

Obsidian is a naturally occurring volcanic glass that was utilized by peoples worldwide to produce stone tools and decorative objects. In South America, obsidian occurs along the volcanic arc of the Nazca subduction zone of the central Andes and was utilized by prehistoric peoples beginning in the Terminal Pleistocene over 12,000 years ago (Rademaker *et al.* 2014; Sandweiss *et al.* 1998; Yataco and Nami 2016). Andean obsidian deposits vary in respect to glassiness; inclusions; size of nodules and pyroclasts; color(s) ranging from black, red, brown, green, and multicolored banded or mottled; and opacity (Glascock *et al.* 2007). Such attributes can vary greatly even within the same geologic source area (e.g., Rademaker *et al.* 2013, 2021). Although Andean obsidian sources cannot be distinguished solely based on macroscopic qualities, geochemical analyses have demonstrated that ratios of trace elements are unique to each obsidian source and can be used to characterize obsidian artifacts (Burger and Asaro 1977, 1979; Glascock *et al.* 2007). Artifact provenance studies show that three major geologic sources were predominantly exploited in the central Andes corresponding to Quispisisa, Alca, and Chivay obsidians (Figure 9.1). Over the last four decades, exploration of highland zones in the central Andes have identified and mapped these major obsidian deposits (Brooks *et al.* 1997; Burger *et al.* 1998a, 1998b; Burger and Glascock 2002; Jennings and Glascock 2002; Rademaker *et al.* 2013, 2021; Tripcevich 2007; Tripcevich and Contreras 2011).

Archaeological Context

This study examines a Middle Horizon (AD 600–1000) obsidian assemblage recovered from the upper Majes Valley in the department of Arequipa, Peru. During the Middle Horizon, obsidian was transported to its greatest extent across the Andes (Burger *et al.* 2000). This is in part due to the expansion of large-scale polities and states including the Wari empire, whose capital was located in Peru's highland Ayacucho Valley (Figure 9.1); and Tiwanaku, whose ceremonial capital was founded in the Titicaca Basin of Bolivia. At this time, residents of what is now the department of Arequipa adopted foreign styles, prestige items, and practices linked to such foreign groups. The emergence of inter-valley roads and caravan waystations at major confluences between Arequipa's coastal valleys provide evidence of the increasing scales of regional connectivity and economic exchange during the Middle Horizon (Cardona 2002; Jennings *et al.* 2015; Nigra *et al.* 2017; Tung 2012). As Arequipa was located at the crossroads of both Wari and Tiwanaku interests, provenance studies of obsidian allow us to investigate how local and exotic materials were utilized by communities located along coast-highland corridors.

In 2017, Reid (2020) conducted archaeological excavations at four Middle Horizon sites in the upper Majes Drainage and Chuquibamba Tributary under the auspices of the Proyecto Arqueológico Caminos Preincaicos Arequipa (PACPA). All four sites are located on the same prehistoric road artery that connects the Majes River Valley to the upper Chuquibamba drainage and adjacent highland zones (Figure 9.2). Two of these sites, Pakaytambo and El Tambo, correspond to an intrusive Wari occupation in the valley. Located at ~1700 masl, Pakaytambo is a small Wari enclave with orthogonal patio-groups organized around a monumental platform (35m × 60m) on top of which sits a D-shaped temple enclosure. Associated radiocarbon dates range from AD 770–990 (calibrated, SHCal20)[2] showing that this Wari temple center was first constructed in the latter half of the Middle Horizon during the apex of Wari expansionism.

El Tambo is an adjacent state center located under one km to the south that was built at the same time, if not earlier, than Pakaytambo. The site contains large bounding walls that enclose a large plaza (45m × 50m) and adjoining rectilinear compounds. Surface ceramics indicate that the site was repurposed by the Inka state who likely replicated Wari state strategies in the valley. Both the Wari and Inka took control of the natural chokepoint and transit route in the upper drainage between population centers in the Chuquibamba basin and those in the Majes Valley below.

Founded by local inhabitants of the Majes culture area, the waystations and ceremonial centers of Santa Rosa II (~1060 masl) and La Angostura (~1130 masl) are likely contemporaneous with the Wari occupation in

[2] All radiocarbon dates were calibrated using Hogg *et al.* 2020.

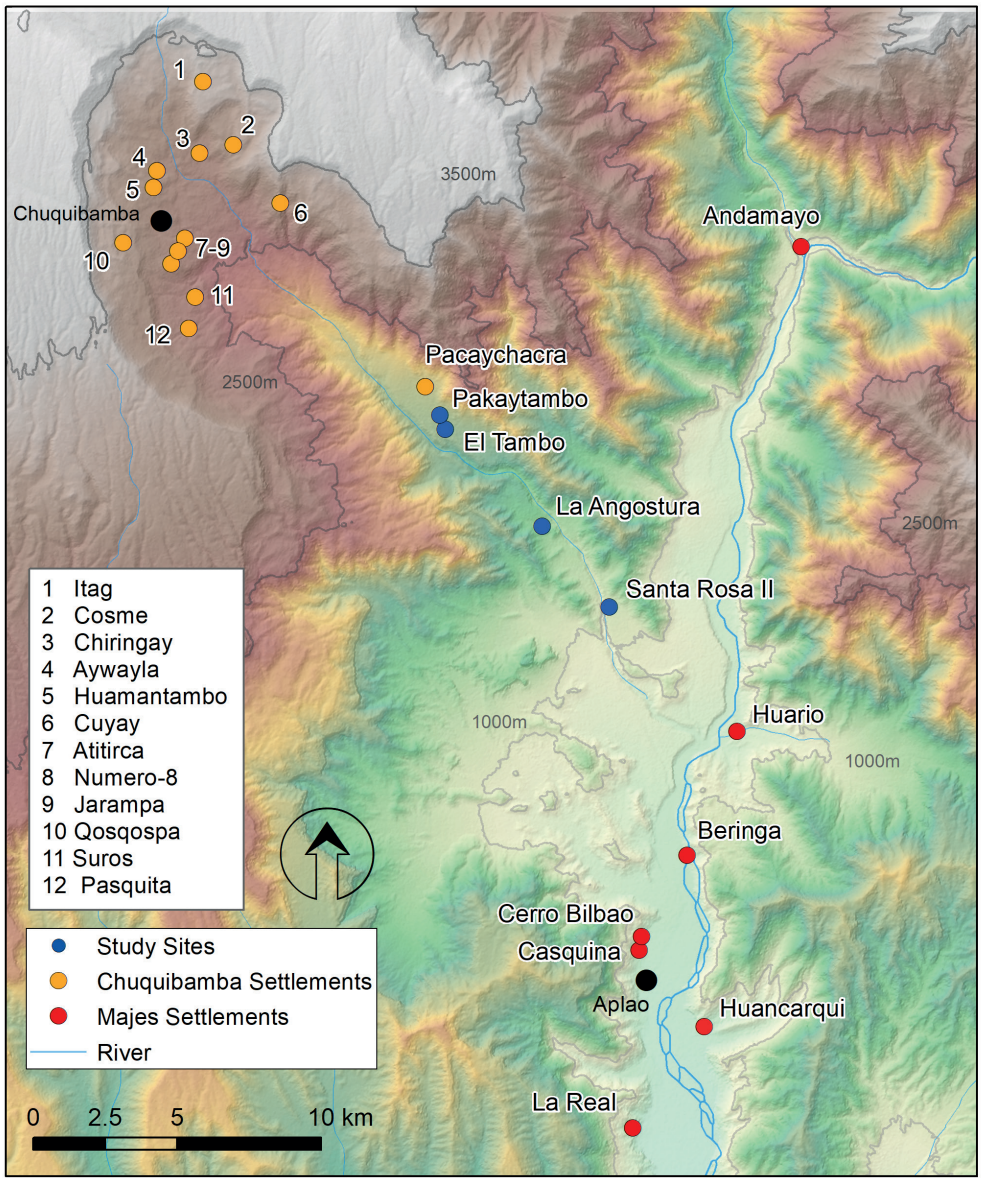

Figure 9.2. Map of study area with archaeological sites.

the upper valley. Santa Rosa II was first recorded by García and Bustamante (1990: 32–34) who noted the site's function as a caravan waystation at the drainage's major highland-coast confluence in the Majes. The site is organized around a large square plaza (67m × 67m) with an adjoining complex abutting the northern wall composed of rectilinear rooms and open patio spaces. This site layout is replicated in smaller form at La Angostura, only four kilometers away (Reid 2020). Both sites show local patterns of architecture, construction practices, and material culture that includes Wari-influenced ceramic forms and designs. In the surrounding vicinities of the formal plaza complexes, numerous corrals and the irregular stone footings of small structures are found, likely utilized by caravans and periodic residents. Materials also show long-distance connections including marine shell and petrified wood from the coast and obsidian from highland regions. Marking both sites are elaborate geoglyphs that include the forms of concentric circles, sun motifs, and other geometric designs, observable from nearby ridges and prehistoric trails.

The establishment of road and waystation infrastructure by local communities may have been one strategy of local elites to coopt an increase in caravan activity linked to the Wari state presence in Arequipa. As practices of ideology are embedded within exchange systems, Santa Rosa II and La Angostura also served as central places for large-scale gatherings perhaps linked

to periodic festivals, barter fairs, and/or religious activities. At all sites, obsidian is abundant and present across most excavation units. Obsidian was mapped in-situ when observed during excavations and recovered through fine-screening of excavated sediments. The majority of obsidian specimens correspond to flaked stone tool debris and was recovered alongside other domestic refuse.

Obsidian Assemblage and Attributes

A total of 303 obsidian artifacts were analyzed in Peru by pXRF that complemented a formal lithic analysis of materials (Reid 2020). Complete obsidian tools include a core (n=1), preform (n=1), biface (n=1), scraper (n=1), blades (n=2), drills (n=3), projectile points (n=16), and biface/uniface fragments (n=36) that include the tips, medial sections, and bases of broken points (Table 9.1). Debitage large enough for pXRF analysis included complete and broken flakes (n=194) in addition to small bifacial thinning flakes (n=12) and shatter (n=36). This chapter focuses on these debitage materials, some of which show evidence of use wear likely related to expedient flake use.

Type	Count (N)
Biface	1
Projectile Point	16
Biface/Uniface Fragment	36
Blade	2
Core	1
Preform	1
Drill	3
Scraper	1
Flake	194
Bifacial thinning flake	12
Shatter	36
Total	303

Table 9.1. Number of obsidian artifacts characterized by pXRF by lithic type.

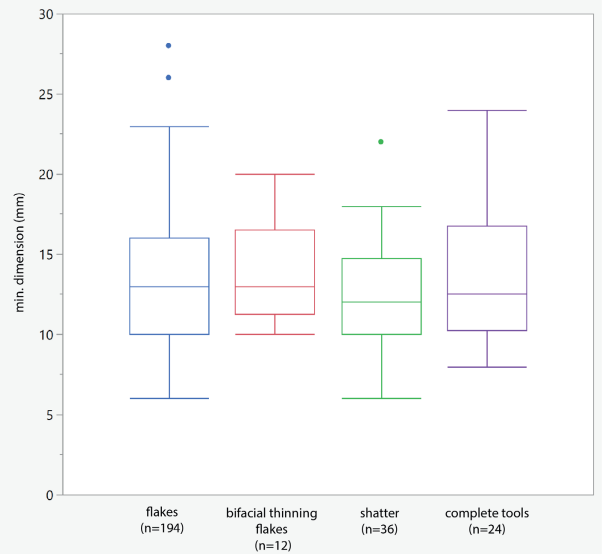

Figure 9.3. Size plots (minimum dimension of length or width) by artifact type analyzed by pXRF. Center line shows the mean with outlier indicated by individual points.

Specimen Size

Lithic artifact size is defined by several measurements including length, width, thickness, and weight. During the 2017 excavations, all soil was dry screened through fine mesh (1/16th inch or ~1.7mm), allowing for the recovery of micro-debitage measuring < 0.1g in weight. For flakes, length (mm) was measured as the straight-line distance perpendicular to the striking platform, otherwise from proximal to distal ends. Width (mm) and thickness (mm) were measured at their maximum dimensions. Weight (g) is also reported here as it is a key measurement related to the stage of lithic production. As a general practice, specimens that could fit over the instrument's aperture window were analyzed regardless of thickness or weight. Of the total obsidian assemblage recovered by the PACPA investigation, 65% was analyzed by pXRF. The remaining artifacts correspond to micro-debitage and were too small to fit over the instrument aperture.

Specimen size can greatly impact pXRF measurement accuracy if the sample does not fully cover the X-ray beam. For example, Liritzis (2008) shows systematic differences in ppm concentrations based on the percent coverage of the sample over the aperture window and uses this ratio to correct for size. In the current study, the aperture window of the instrument has a diameter of 10mm. As per Figure 9.3, only a handful of specimens did not completely cover the window. However, surface irregularities of debitage also impact X-ray beam coverage as not all specimens contain planar surfaces that can be placed flush with the aperture window. This was especially true for obsidian shatter.

Specimen Thickness

XRF analyses are also impacted by the thickness of a sample or specimen. This relates to the principle of "infinite thickness" or the sampling depth where all X-rays are absorbed and accurate readings are possible. Samples that are infinitely thick meet the critical point where increasing the thickness would not impact the measurement whether it be by 1mm or infinite mm. If X-ray penetration depth is greater than the thickness of the sample, the specimen cannot fully

contain the X-ray beam or emit characteristic X-rays to accurately calculate an elemental quantity from a given (Frahm 2016: 450; Shackley 2011: 215). Various studies have attempted to determine the minimum thicknesses of obsidian samples needed for accurate source characterization. Infinite thickness differs per element. Davis *et al.* (2011: 61) observe that for mid-Z elements (Rb_{37} through Nb_{41} including elements of interest Rb, Sr, Y, Zr), minimum sample thickness ranges between 1.2 to 2.5mm. Other investigators suggest a cut-off at 2mm thickness (Shackley 2012).

Of the analyzed obsidian artifacts in this study, only a handful of flakes fall short of a 2mm thickness. By artifact type, lithic shatter tended to have greater thicknesses than flakes and complete tools (Figure 9.4). Specimens were placed over the aperture at their thickest points while also covering the entire beam window. However, it should be noted that only maximum thickness measurements were taken on artifact samples and thus do not account for the tapering thicknesses of most flakes, where the maximum thickness is associated with the bulb of force that forms below the striking platform. Various investigators have tested methods to correct for thin specimens such as the use of a small beam analyzer and normalization to the Compton peak (Ferguson 2012) or by taking the ratios between spectral peaks (Hughes 2010) and ppm concentrations (Frahm 2016).

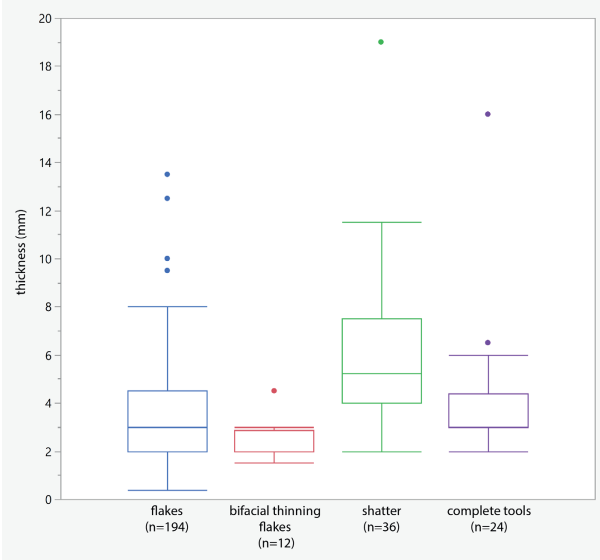

Figure 9.4. Thickness (mm) plots by artifact type analyzed by pXRF.

Specimen Weight

Weight is also a key measurement in lithic studies as it correlates to other linear dimensions and stage of lithic reduction (Shott 1994: 80). Of the analyzed obsidian artifacts, it is not surprising that the greatest weights are associated with complete tools followed by shatter, flakes, and then bifacial thinning flakes (Figure 9.5). Despite several outliers, the artifacts analyzed in this study are relatively small in size as reflected in minimum dimension, thickness, and weight. This is likely related to the precious nature of obsidian and distance from the source compared to more readily available local cherts and quartzes which show the greatest evidence of primary reduction at the study sites themselves (Reid 2020).

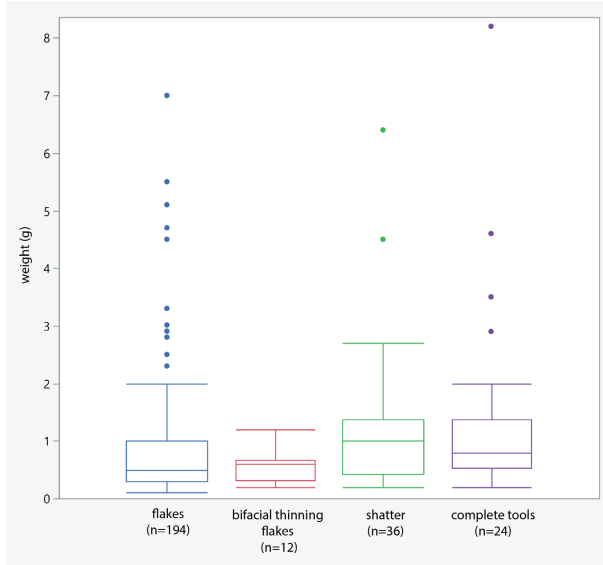

Figure 9.5. Weight (g) plots by artifact type analyzed by pXRF.

Methods

Analyses were conducted in Peru during the summers of 2017 and 2018 using a Thermo Scientific Niton XL3t Goldd+ portable X-ray Fluorescence (pXRF) instrument. The device is equipped with a 50kV silver anode tube with a Geometrically Optimized Large Area Drift Detector (GOLDD). Specimens were analyzed under "Test All Geo" mode using the settings of Main (40kV and 100µA), Low (25kV and 100µA), Light (15kV and 200µA), and High (50kV and 100µA) each set for 30 seconds for a total analysis run time of 120s per sample. Samples were subsequently analyzed using the instrument's "Soils" mode as it has been shown to provide more accurate results for concentrations of the element rubidium (Rb) above 150 parts-per-million (ppm). Filters under Soils mode were set on Main, Low, Light, and High for 30s each for a total run time of 120s. Samples were placed on the instrument aperture along their thickest and most planar surface to fully cover the X-ray beam detector field. Surfaces with cortex and evidence of devitrification were

Table 9.2. Relative standard deviation (RSD) over a two-year instrument operating period.

ID	n	Ti	Mn	Fe	Zn	Rb	Sr	Y	Zr	Nb	Ba	Pb	Th
CRB-2005	17	7.4	9.8	1.2	2.5	3.3	n.a.	3.5	3.5	2.9	n.a.	4	6.1
ELC-001	18	4.9	13.5	5.2	9.8	2.8	3.2	13.1	10.9	11.6	25.1	15.2	28.3

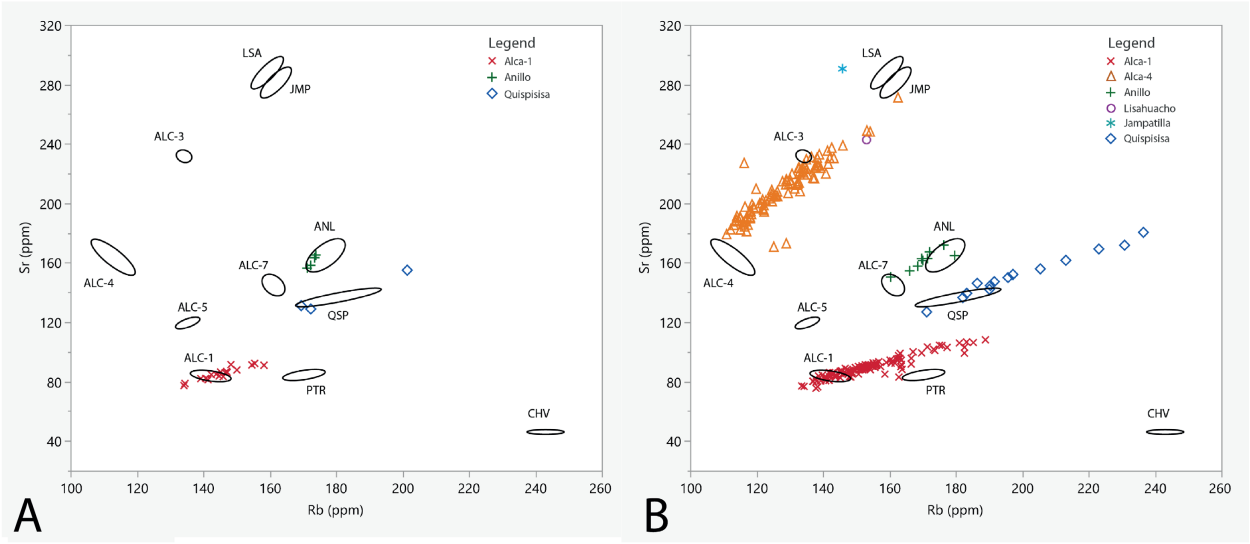

Figure 9.6. Bivariate plot of strontium (Sr) versus rubidium (Rb) concentrations measured by pXRF (ellipses drawn at 95% confidence around geologic source groups). A) Complete tools only; B) Debitage only.

avoided. Trace element data are reported in ppm for a total of 13 elements, including: potassium (K), calcium (Ca), titanium (Ti), manganese (Mn), iron (Fe), zinc (Zn), rubidium (Rb), strontium (Sr), yttrium (Y), zirconium (Zr), niobium (Nb), lead (Pb), and thorium (Th), however only a subset of these prove useful to discriminate Andean obsidians.

Collected data were then calibrated using a specialized correction developed by Mark Golitko (University of Notre Dame) using 21 in-house and certified standards including NIST 610, NIST 612, and Glass Buttes and Sierra Pachuca obsidians (see Glascock 1999). During field analyses, two obsidian standards were run at the beginning and end of each day to track instrument precision and variation over time. The two obsidian samples correspond to the Cedar Butte #2 source located in the Snake River Valley, Idaho (CRB2005) and El Chayal in Guatamala (ELC001). As indicated by the relative standard deviation (RSD), there was a high instrument precision/reproducibility (< 10% RSD) throughout the analysis especially for the elements of interest rubidium (Rb) and strontium (Sr) (< 3.3% RSD) (Table 9.2).

Despite data calibration using international standards, inter-instrumental comparisons of pXRF data can prove problematic, making source assignments to previously published elemental values unreliable (Frahm 2013; Shackley 2010; Speakman and Shackley 2013). To assign artifacts to their respective character groups (related to known or unknown geologic sources), we followed a rigorous statistical approach following Glascock *et al.* (1998). In addition, geologic samples collected from central Andean obsidian sources were measured on the Niton XL3t Goldd+ pXRF under the same instrumental settings. Geologic obsidians were loaned or donated to the Field Museum's Elemental Analysis Facility by Kurt Rademaker, Nicholas Tripcevich, and Michael Glascock for use in this study. After the calibration of raw artifact and geologic data, ppm values were log10 transformed for statistical analyses using the software JMP Pro v15.2.0.

Results

Obsidian Group Characterization: Multivariate Analyses

Here we present the elemental ppm concentrations of the analyzed obsidian artifacts from the upper Majes Valley and Chuquibamba Tributary. Due to the overall small size of the measured artifacts, elemental concentrations are likely over-estimated for small specimens. This may initially seem counter-intuitive, as when a sample is too small to fully cover the aperture or does not meet the infinite thickness

for an element of interest, one might expect a relative deficit in X-rays bombarding the sample that would result in lower elemental intensities. However, our findings mirror those of Frahm (2016: 451), who also utilized a Niton XL3t Goldd+ analyzer and found that trace element concentrations tend to *increase* as specimen size *decreases* for samples measured with only air surrounding them. This is likely due to an underestimation of mass for small samples within the internal fundamental parameter (FP) algorithm used to calculate the ppm concentrations under the "Test-all Geo" mode.

Prior analyses using the Niton XL3t Goldd+ have shown that for samples with concentrations of Rb higher than 150ppm, "Soils" mode is ideal. In this mode, the internal software of the instrument uses the Compton peak for the determination of mass/volume normalization. For small specimens, a smaller fraction of the higher energy X-rays will interact with the sample (i.e., volume or mass) exposed to the beam. But the lower energy X-rays which have a shorter range are more likely to interact and return a signal to the detector. Since the instrument's software uses the Compton peak (higher energy X-rays) for the mass/volume normalization, this explains why lower Z elements (Fe, Zn, Rb) are more inflated than higher Z elements (Zr). The overestimation of Rb concentrations under "Soils" mode can prove problematic as this element (alongside Sr) is most commonly used to distinguish Andean obsidians using pXRF (Glascock *et al.* 2007).

The relationship between size and an overestimation of ppm elemental concentrations within the Majes obsidian materials is clearly identified when comparing debitage versus complete obsidian tools. A scatterplot of Sr versus Rb ppm concentrations for complete obsidian tools fall within or close to geologic ellipses produced from measurements of geologic samples analyzed using the same Niton XL3t Goldd+ instrumentation and settings (Figure 9.6A). However, for small-sized debitage, character groups display long tails at their extremes due to the overestimation of ppm values for Rb (Figure 9.6B). Complicating the picture, several assigned character groups overlap with more than one geologic source when considering only Sr versus Rb concentrations. Consequently, we cannot rely on the traditional Sr versus Rb scatterplot alone for geochemical group characterization of the Majes obsidian materials. This necessitated a more robust approach using several multivariate analyses to accurately characterize small-sized obsidian debitage.

Initial artifact character groups were created based on a Ward's hierarchical cluster analysis using the

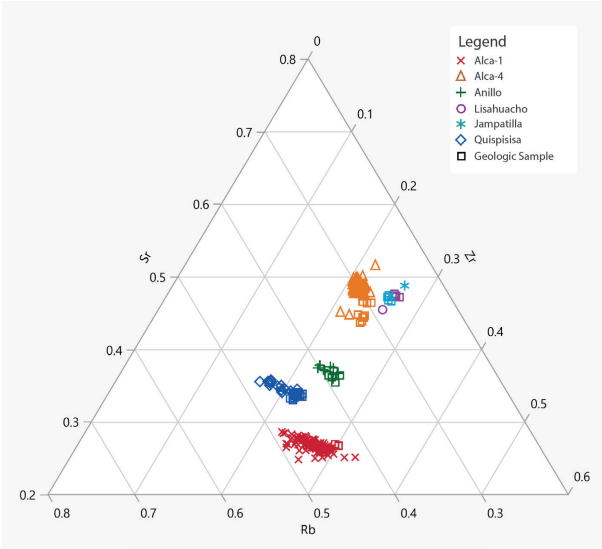

Figure 9.7. Ternary plot of strontium (Sr), rubidium (Rb), and zirconium (Zr) for obsidian debitage.

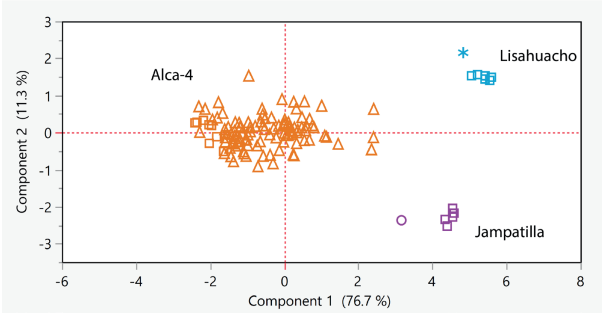

Figure 9.8. Principal component analysis (PCA) of elements Rb, Sr, Y, Zr, and Th.

elements Sr, Rb, and Zr. These groups were then interrogated using various methods. One alternative to bivariate scatterplot visualizations is the use of ternary plots, or three-axis plots, where ppm concentrations are converted into proportions for each sample. Here a ternary plot between Sr, Rb, and Zr more clearly defines the character groups of the Majes debitage materials (Figure 9.7). Multivariate analyses have also been shown to reduce the skewing effects of sample size. For example in principal component analysis (PCA), multiple elemental concentrations can be reduced to their underlying covariances typically inspected through the first two principal components (Glascock *et al.* 1998). As an initial step, PCA is useful for identifying discriminating elements of interest for further multivariate comparisons. Here we present the results of a PCA using logged elemental ppm concentrations of Rb, Sr, Y, Zr, and Th which distinguishes the obsidian groups Alca-4, Lisahuacho, and Jampatilla (Figure 9.8).

Previous investigations have illustrated the use of elemental ratios of ppm concentrations (Frahm 2016)

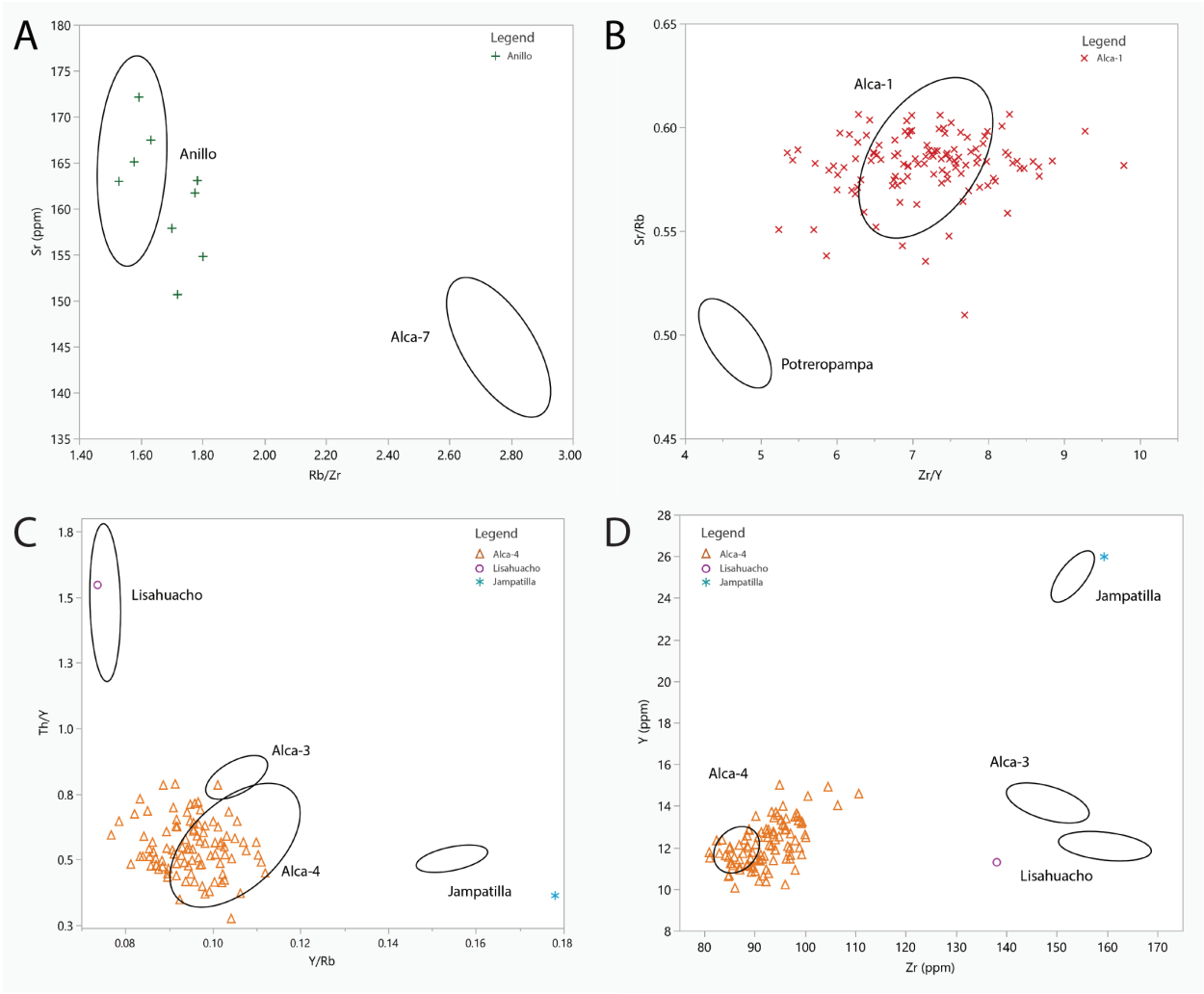

Figure 9.9. Bivariate plots of obsidian debitage element concentrations measured by pXRF (ellipses drawn at 95% confidence around geologic source groups). A) Anillo versus Alca-7 using Sr and ratio Rb/Zr; B) Alca-1 versus Potreropampa using ratio Sr/Rb versus Zr/Y; C) Alca-4 versus Alca-3, Lisahuacho, and Jampatilla using ratio Th/Y and Y/Rb; and D) Y versus Zr.

and peak intensities (Hughes 2010) in the analysis of small-sized obsidian debitage. The underlying premise is that if artifact size systematically impacts all mid-Z trace elements, then converting ppm concentrations or spectral peak values into elemental ratios will mitigate any disproportional skewing. Most notably, Frahm (2016) illustrates how very small obsidian fragments can be accurately sourced in a reexamination of historic pXRF and energy-dispersive (ED)-XRF datasets as well as experimental materials of varying size. For one obsidian group, Frahm (2016: 458) was able to reduce the relative standard deviation (RSD) corresponding to Sr from 14% down to 3–4% when ratioing Sr concentrations with Rb, Nb, and Zr.

Due to the proximity of some Andean geologic groups when comparing only Sr versus Rb, we can use the ratios between various elements of interest to aid in group characterization. Ratios of Rb/Zr versus Sr best distinguishes Anillo from Alca-7 (Figure 9.9A), and Sr/Rb versus Zr/Y further distinguishes Alca-1 from Potreropampa (Figure 9.9B). Ratios also confirmed the presence of Lisahuacho and Jampatilla obsidian within the assemblage (Figure 9.9C-D). Both artifacts pertain to small flakes and represent the first evidence of these sources in the department of Arequipa. Discriminant analysis was also used in tandem with multivariate analyses to test these character groups (Figure 9.10).

Character Group Assignment

Our results indicate the presence of six discrete geologic obsidian sources utilized by occupants of the upper Majes Valley and Chuquibamba Tributary during the Middle Horizon. These correspond to the local Arequipa obsidian groups Alca-1, Alca-4, and Anillo as

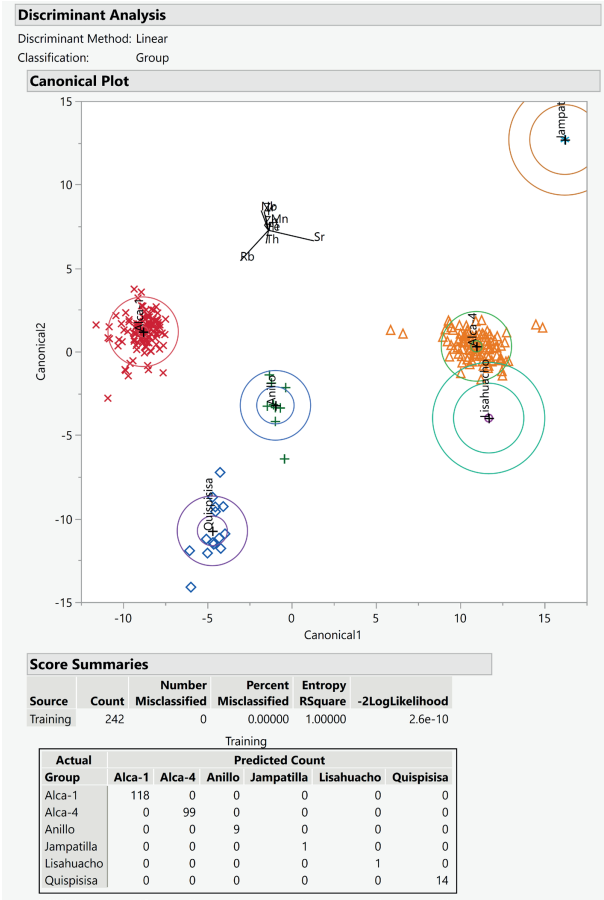

Figure 9.10. Results of discriminant analysis using the elements: Ti, Mn, Fe, Zn, Rb, Sr, Y, Zr, Nb, and Th.

well as exotic obsidians including Quispisisa, Jampatilla, and Lisahuacho from the south-central highlands of Ayacucho and Apurímac (Figure 9.1). In this chapter we present both the count (Table 9.3) and weight (Table 9.4) of analyzed specimens. This is an important practice as reporting only counts can over-emphasize the presence of an obsidian source. Hypothetically, by count, ten small retouch flakes of Source A outnumber one large biface of Source B, however by weight the reverse may be true. Following regional trends, Alca-1 is the predominant obsidian comprising nearly half of analyzed debitage by count and weight. This is followed closely by Alca-4 (41%), whereas small amounts of Anillo (7%) and Quispisisa (3%) were also detected. Lisahuacho and Jampatilla represent < 1% of the assemblage by count and weight represented by a single flake from each source.

Discussion

The use of pXRF instrumentation in the field allows investigators to analyze entire obsidian assemblages in a relatively rapid, inexpensive, and non-destructive manner. For this study, specimens that could fit over the X-ray beam aperture (10mm diameter) of the Niton XL3t Goldd+ pXRF were measured. Variation in specimen size, thickness, and surface irregularity did impact the accuracy of pXRF results for small-sized debitage where ppm concentrations are likely overestimated. However, following prior studies (e.g., Frahm 2016), the use of multivariate analyses and the ratioing of elemental concentrations allowed for accurate obsidian source characterization in direct comparison to geologic materials. Following these results, future studies may attempt to further push size limits to include microdebitage. For example, in this case study, microdebitage corresponded to roughly one third of the archaeological obsidian assemblage however these specimens were not analyzed. Especially difficult specimens to characterize could then be targeted for export for analysis by traditional XRF, INAA, or LA-ICP-MS (e.g., Kellett *et al.* 2013).

The use of pXRF allows for wider detection of rare and exotic obsidian sources that may only comprise < 1% of the total assemblage. During the Middle Horizon, there

Table 9.3. Geologic source characterization of obsidian debitage by count (N).

Type by count (N)	Alca-1	Alca-4	Anillo	Lisahuacho	Jampatilla	Quispisisa	Total
Flake	97 (47.1%)	85 (41.3%)	9 (4.4%)	1 (0.5%)	1 (0.5%)	13 (6.3%)	206 (85.1%)
Shatter	21 (58.3%)	14 (38.9%)	0	0	0	1 (2.8%)	36 (14.9%)
Total	118 (48.8%)	99 (40.9%)	9 (3.7%)	1 (0.4%)	1 (0.4%)	14 (5.8%)	242 (100%)

Table 9.4. Geologic source characterization of obsidian debitage by weight (g).

Type by weight (g)	Alca-1	Alca-4	Anillo	Lisahuacho	Jampatilla	Quispisisa	Total
Flake	79.6 (48.0%)	63.2 (38.1%)	15.3 (9.2%)	0.3 (0.2%)	0.9 (0.5%)	6.6 (4.0%)	165.9 (79.1%)
Shatter	20.3 (46.2%)	23.4 (53.3%)	0	0	0	0.2 (0.5%)	43.9 (20.9%)
Total	99.9 (47.6%)	86.6 (41.3%)	15.3 (7.3%)	0.3 (0.1%)	0.9 (0.4%)	6.8 (3.2%)	209.8 (100%)

is strong evidence that obsidian bifaces and projectile points were transported and exchanged over great distances in completed form where initial production occurred off-site (Bencic 2000; Burger *et al.* 2000). Since formal tools are not always deposited at the place of their production, often only the smallest retouch flakes related to periodic maintenance and sharpening of a tool's edge may be archaeologically recovered. In this case study, this is exemplified by the presence of a single bifacial thinning flake composed of Lisahuacho obsidian. It is therefore critical that studies include small obsidian debitage within geochemical provenance studies in order to best detect the diversity of obsidian usage in the past (e.g., Eerkens *et al.* 2007).

PXRF analysis of obsidian debitage from the upper Majes Drainage provides greater insight into prehistoric regional economies and long-distance interactions related to the broader social transformations of the Andean Middle Horizon. The use of the local obsidians Alca-1, Alca-4, and Anillo show a well-integrated highland-montane valley network in the proximate region, whereas the presence of Quispisisa, Jampatilla, and Lisahuacho provide evidence of long-distance interaction with the south-central highlands of Peru. The heterogeneity of the Alca source region (Rademaker *et al.* 2013, 2021) also allows us to pin-point the locations of obsidian extraction on the local landscape. From the rim of the Chuquibamba basin, Alca-4 is the nearest high quality bedrock source accounting for its near equal presence alongside Alca-1 in total analyzed artifacts in this analysis (Figure 9.1). This study is also one of the first investigations to detect the prehistoric use of Anillo obsidian. The Anillo source is located on the western side of the Cotahuasi Valley in close proximity to a major caravan route that links Arequipa to Apurímac and Ayacucho (Tripcevich 2016).

Minor amounts of Quispisisa obsidian are also present in the upper Majes Valley at the study sites Santa Rosa II and La Angostura. At other settlements in Arequipa and Moquegua, Quispisisa comprises ~10–20% of sourced obsidian assemblages (Glascock 2012; Rizzuto and Jennings 2021; Tung 2012; Williams *et al.* 2010, 2012). Quispisisa is commonly associated with Wari exchange networks as it was the preferred obsidian source of the Wari state (Burger *et al.* 2000). Analysis of small-sized obsidian debitage further allowed for the characterization of the exotic sources Jampatilla and Lisahuacho originating in the departments of Ayacucho and Apurímac respectively. These sources are found enroute from the Wari heartland to the Majes Drainage, and this study is the first to detect their presence in Arequipa. In consideration of lithic tool type, 72.7% of exotic non-Arequipa obsidians analyzed in this study are debitage, the majority of which correspond to late-stage production or maintenance. For example, the only specimen assigned to Lisahuacho is a small bifacial thinning flake, suggesting exotic obsidians were transported into the region as already completed tools or near-finished products, perhaps as trade items.

Obsidian is only one material good among many that would have been transported across caravan routes between highland and coastal zones. The minor presence of exotic obsidians, including single objective flakes, can be interpreted as one-off or random finds; however, they can play a critical role in reconstructing down-the-line exchange networks and serve as proxies to reconstruct broader social networks (e.g. Golitko *et al.* 2012). Obsidian provenance data, alongside other lines of material evidence such as prehistoric roads, suggest that a Middle Horizon caravan route once linked Wari Ayacucho to far southern Peru, likely connected by various waystation sites such as Santa Rosa II and La Angostura. This route would have extended from Ayacucho into Apurímac with travel southward, crossing the Cotahuasi Valley near the Anillo obsidian source, and entering the upper Majes Drainage near Chuquibamba.

Caravan activity was facilitated by both local populations in the Majes Drainage and an intrusive Wari state. State enclaves at the sites Pakaytambo and El Tambo were established at the natural chokepoint in the valley to perhaps control this major travel route. Obsidians local to Arequipa also flowed in the opposite direction, including small amounts of Alca-1 identified at the Wari administrative center Jincamocco, the Wari capital, and Espíritu Pampa on the eastern Andean slopes (Burger *et al.* 2000; Fonseca and Bauer 2020; Kaplan 2018; Schreiber 1992). The obsidian data support initial models of Wari travel routes in southern Peru (Williams 2009) and the survey of Middle Horizon roads in Arequipa (Cardona 2002).

Conclusion

This study demonstrates the reliability of pXRF for the analysis of small sized obsidian debitage. Various multivariate methods are suggested to mitigate factors of debitage size, thickness, and surface irregularity that negatively impact measurement accuracy. These include hierarchical cluster analysis, ternary graphing, principal component analysis, ratioing elemental ppm concentrations, and discriminant analysis in direct comparison to representative geologic samples. Our results indicate an accurate characterization of Andean obsidian artifacts with minimum dimensions as small as 0.6mm in size, 0.5mm thickness, and 0.1g in weight.

The characterization of rare and exotic obsidian sources that comprise < 1% of the overall artifact assemblage highlights the importance of including small debitage

within geochemical analyses. Obsidian was often exchanged and transported as completed tools and bifaces. Various archaeological processes may result in the final use or discard of such tools off-site at the end of their operational lifetime. Thus, small flaked debitage related to periodic tool maintenance may best indicate the range and presence of exotic obsidians. In this case study, such small sized debitage allows us to elucidate the provisioning of obsidian materials from both local and intrusive state contexts. The sourcing of obsidian artifacts from road waystations also highlights the role of long-distance llama caravans in the movement of this precious material from highland sources to the coastal valleys of the Andes during the Middle Horizon period.

Acknowledgements

Investigations were permitted by the Peruvian Ministry of Culture (Resolution N°234-2017-DGPA-VMPCIC/MC). We would like to thank PACPA codirector Lidia Betsabe Camargo Padilla and Elizabeth J. Olson for their assistance in Peru and acknowledge the assistance of Mark Golitko and Laure Dussubieux at the Elemental Analysis Facility at The Field Museum of Natural History, which has been funded by the W.W. Grainger Foundation, the Negaunee Foundation, and the National Science Foundation (BCS-1628026, 1531394, 1321731, 0818401, and 0320903). Two anonymous reviewers also provided helpful and insightful commentary on these findings.

Bibliography

Andrefsky, W. 1994. Raw-material availability and the organization of technology. *American Antiquity* 59(1): 21–34.

Andrefsky, W. 2007. The application and misapplication of mass analysis in lithic debitage studies. *Journal of Archaeological Science* 34(3): 392–402.

Bélisle, V., H. Quispe-Bustamante, T.J. Hardy, A.R. Davis, E. Antezana Condori, C. Delgado González, J.V. Gonzales Avendaño, D.A. Reid, and P.R. Williams 2020. Wari impact on regional trade networks: patterns of obsidian exchange in Cusco, Peru. *Journal of Archaeological Science: Reports* 32: 1–10.

Bencic, C.M. 2000. Industrias líticas de Huari y Tiwanaku. *Boletín de Arqueología PUCP* 4: 89–118.

Brooks, S.O., M.D. Glascock, and M. Giesso 1997.Source of volcanic glass for ancient Andean tools. *Nature* 386: 449–50.

Burger, R.L. and F. Asaro 1977. *Trace Element Analysis of Obsidian Artifacts from the Andes: New Perspectives on Prehispanic Economic Interaction in Peru and Bolivia – LBL6343*. Berkeley (CA): Lawrence Berkeley Laboratory.

Burger, R.L. and F. Asaro 1979. Análisis de Rasgos Significativos en la Obsidiana de los Andes Centrales. *Revista del Museo Nacional* 43: 281–325

Burger, R.L., F. Asaro, P. Trawick, and F. Stross 1998a. The Alca obsidian source: the origin of raw material for Cuzco type obsidian artifacts. *Andean Past* 5: 185–202.

Burger, R.L., F. Asaro, G. Salas, and F. Stross 1998b. The Chivay obsidian source and the geological origin of Titicaca Basin type obsidian artifacts. *Andean Past* 5: 203–23.

Burger, R.L., and M.D. Glascock 2002. Tracking the source of Quispisisa obsidian from Huancavelica to Ayacucho, in W.H. Isbell and H. Silverman (eds) *Andean Archaeology I: Variations in Sociopolitical Organization*: 341–68. New York (NY): Kluwer Academic/Plenum Publishers.

Burger, R.L., K.L. M. Chávez, and S.J. Chávez 2000. Through the glass darkly: Prehispanic obsidian procurement and exchange in southern Peru and northern Bolivia. *Journal of World Prehistory* 14(3): 267–362.

Cardona Rosas, A. 2002. *Arqueología de Arequipa: De Sus Albores a los Incas*. Arequipa: CIARQ.

Craig, N., R.J. Speakman, R.S. Popelka-Filcoff, M.D. Glascock, J.D. Robertson, M.S. Shackley, and M.S. Aldenderfer 2007. Comparison of XRF and PXRF for analysis of archaeological obsidian from southern Perú. *Journal of Archaeological Science* 34(12): 2012–24.

Davis, M.K., T.L. Jackson, M.S. Shackley, T. Teague, and J.H. Hampel 2011. Factors affecting the energy-dispersive X-ray fluorescence (EDXRF) analysis of archaeological obsidian, in M.S. Shackley (ed.) *X-Ray Fluorescence Spectrometry (XRF) in Geoarchaeology*: 45–63. New York (NY): Springer.

Eerkens, J.W., J.R. Ferguson, M.D. Glascock, C.E. Skinner, and S.A. Waechter 2007. Reduction strategies and geochemical characterization of lithic assemblages: a comparison of three case studies from western North America. *American Antiquity* 72(3): 585–97.

Ferguson, J.R. 2012. X-ray fluorescence of obsidian: approaches to calibration and the analysis of small samples, in A.N. Shugar and J.L. Mass (eds) *Handheld XRF for Art and Archaeology*: 401–22. Leuven: Leuven University Press.

Fonseca, J. and B.S. Bauer (eds) 2020. *The Lord of Vilcabamba and the Wari Enclave of Espíritu Pampa*. Los Angeles (CA): Cotsen Institute of Archaeology Press.

Frahm, E. 2013. Is obsidian sourcing about geochemistry or archaeology? a reply to Speakman and Shackley. *Journal of Archaeological Science* 40(2): 1444–48.

Frahm, E. 2016. Can I get chips with that? sourcing small obsidian artifacts down to Microdebitage scales with portable XRF. *Journal of Archaeological Science: Reports* 9: 448–67.

Garcia Márquez, M., and R. Bustamente Montoro 1990. Arqueología Del Valle de Majes. *Gaceta Arqueológica Andina* 18(19): 25–40.

Giesso, M., H.G. Nami, J.J. Yataco Capcha, M.D. Glascock, and B.L. MacDonald 2020. XRF obsidian analysis from Ayacucho Basin in Huamanga province, South-Eastern Peru. *Archaeometry* 62(2): 215–31.

Glascock, M.D. 1999.An inter-laboratory comparison of element compositions for two obsidian sources. *International Association for Obsidian Studies Bulletin* 23: 13–15.

Glascock, M.D. 2012.Obsidiana: Síntesis de movilidad giratoria, in W. Yepez and J. Jennings (eds) *Wari en Arequipa: Análisis de los Contextos Funerarios de La Real*: 174–181. Arequipa: Museo Arqueológica José María Morante and Universidad Nacional de San Agustín.

Glascock, M.D., G.E. Braswell, and R.H. Cobean 1998. A systematic approach to obsidian source characterization, in M.S. Shackley (ed.) *Archaeological Obsidian Studies*: 15–65. New York (NY): Plenum Press.

Glascock, M.D., R.J. Speakman, and R.L. Burger 2007. Sources of archaeological obsidian in Peru: descriptions and geochemistry, in M.D. Glascock, R.J. Speakman, and R.S. Popelka-Filcoff (eds) Arch*aeological Chemistry: Analytical Techniques and Archaeological Interpretation*: 522–552. Washington, D.C.: American Chemical Society.

Golitko, M., J. Meierhoff, G.M. Feinman, and P.R. Williams 2012. Complexities of collapse: the evidence of Maya obsidian as revealed by social network graphical analysis. *Antiquity* 86(332): 507–523.

Hogg, A.G., T.J. Heaton, Q. Hua, J.G. Palmer, C.S.M. Turney, J. Southon, A. Bayliss, P.G. Blackwell, G. Boswijk, C.B. Ramsey, C. Pearson, F. Petchey, P. Reimer, R. Reimer, and L. Wacker 2020.SHCal20 southern hemisphere calibration, 0–55,000 years cal BP. *Radiocarbon* 62(4): 759–778.

Hughes, R.E. 1998. On reliability, validity, and scale in obsidian sourcing research, in A.F. Ramenofsky and A. Steffen (eds) *Unit Issues in Archaeology: Measuring Time, Space, and Material*: 103–14. Salt Lake City (UT): University of Utah Press.

Hughes, R.E. 2010. Determining the geologic provenance of tiny obsidian flakes in archaeology using nondestructive EDXRF. *American Laboratory* 42(7): 27–31.

Jennings, J., and M.D. Glascock 2002. Description and method of exploitation of the Alca obsidian source, Peru. *Latin American Antiquity* 13(1): 107–18.

Jennings, J., T.A. Tung, W.J. Yépez Álvarez, G.C. Quequezana Lucano, and M.A. López Hurtado 2015. Shifting local, regional, and interregional relations in Middle Horizon Peru: evidence from La Real. *Latin American Antiquity* 26(3): 382–400.

Kaplan, J. 2018. Obsidian Networks and Imperial Processes: Sourcing Obsidian from the Capital of the Wari Empire, Peru (AD 600–1000). Unpublished PhD dissertation, University of California.

Kellett, L.C., M. Golitko, and B.S. Bauer 2013. A provenance study of archaeological obsidian from the Andahuaylas region of southern Peru. *Journal of Archaeological Science* 40: 1890–1902.

Liritzis, I. 2008. Assessment of Aegean obsidian sources by a portable ED-XRF analyser: grouping, provenance and accuracy, in Y. Facorellis, N. Zacharias, and K. Polikreti (eds) *Proceedings of the 4th Symposium of the Hellenic Society for Archaeometry*: 399–406. Oxford: Archaeopress, BAR International Series.

Matsumoto, Y., J. Nesbitt, M.D. Glascock, Y.I. Cavero Palomino, and R.L. Burger 2018. Interregional obsidian exchange during the Late Initial Period and Early Horizon: new perspectives from Campanayuq Rumi, Peru. *Latin American Antiquity* 29(1): 44–63.

Nazaroff, A.J., K.M. Prufer, and B.L. Drake 2010. Assessing the applicability of portable X-ray fluorescence spectrometry for obsidian provenance research in the Maya Lowlands. *Journal of Archaeological Science* 37(4): 885–95.

Nigra, B.T., A. Cardona Rosas, M.C. Lozada, and H. Barnard 2017. Reconstructing the built environment of the Millo Complex, Vitor Valley, Peru. *Ñawpa Pacha* 37(1): 39–62.

Rademaker, K., M.D. Glascock, B. Kaiser, D. Gibson, D.R. Lux, and M.G. Yates 2013. Multi-technique geochemical characterization of the Alca obsidian source, Peruvian Andes. *Geology* 41(7): 779–82.

Rademaker, K., G. Hodgins, K. Moore, S. Zarrillo, C. Miller, G.R.M. Bromley, P. Leach, D.A. Reid, and D.H. Sandweiss 2014. Paleoindian settlement of the high-altitude Peruvian Andes. *Science* 346(6208): 466–69.

Rademaker, K., M.D. Glascock, D.A. Reid, E. Zuñiga, and G.R.M. Bromley 2021. Comprehensive mapping and compositional analysis of the Alca obsidian source, Peru. *Quaternary International*: 1–16.

Reid, D.A. 2020. Networks of Empire: The Role of Infrastructure in Wari State Expansion in Arequipa, Peru (AD 600–1000). Unpublished PhD dissertation, University of Illinois at Chicago.

Rizzuto, B. and J. Jennings 2021. Quilcapampa's stone tools and Placas Pintadas, in J. Jennings, W. Yépez Álvarez, and S.L. Bautista (eds) *Quilcapampa: A Wari Enclave in Southern Peru*: 258–306. Gainesville (FL): University Press of Florida.

Sandweiss, D.H, H. Mcinnis, R.L. Burger, A. Cano, B. Ojeda, R. Paredes, M. del Carmen Sandweiss, and M.D. Glascock 1998. Quebrada Jaguay: early South American maritime adaptations. *Science* 281(5384): 1830–32.

Schreiber, K.J. 1992. *Wari Imperialism in Middle Horizon Peru* (Vol. 87). Ann Arbor (MI): Museum of Anthropology, University of Michigan.

Shackley, M.S. 2012. Portable X-ray fluorescence spectrometry (PXRF): the good, the bad, and the ugly. *Archaeology Southwest Magazine* 26(2): 1–8.

Shackley, M.S. 2010. Is there reliability and validity in portable X-ray fluorescence spectrometry (PXRF). *The SAA Archaeological Record* 10(5): 17–20.

Shackley, M.S. (ed.) 2011. *X-Ray Fluorescence Spectrometry (XRF) in Geoarchaeology*. New York (NY): Springer.

Shott, M.J. 1994. Size and form in the analysis of flake debris: review and recent approaches. *Journal of Archaeological Method and Theory* 1(1): 69–110.

Speakman, R.J., and M.S. Shackley 2013. Silo science and portable XRF in archaeology: a response to Frahm. *Journal of Archaeological Science* 40(2): 1435–43.

Sullivan, A.P., and K.C. Rozen 1985. Debitage analysis and archaeological interpretation. *American Antiquity* 50(4): 755–79.

Tripcevich, N. 2007. Quarries, Caravans, and Routes to Complexity: Prehispanic Obsidian in the South-Central Andes. Unpublished PhD dissertation, University of California, Santa Barbara.

Tripcevich, N. 2016. The ethnoarchaeology of a Cotahuasi Salt Caravan: exploring Andean pastoralist movement, in J.M. Capriles and N. Tripcevich (eds) *The Archaeology of Andean Pastoralism*: 211–230. Albuquerque (NM): University of New Mexico Press.

Tripcevich, N., and D.A. Contreras 2011. Quarrying evidence at the Quispisisa obsidian source, Ayacucho, Peru. *Latin American Antiquity* 22(1): 121–36.

Tung, T.A. 2012. *Violence, Ritual, and the Wari Empire: A Social Bioarchaeology of Imperialism in the Ancient Andes*. Gainesville (FL): University Press of Florida.

Williams, P.R. 2009. Wari and Tiwanaku borderlands, in M. Young-Sanchez (ed.) *Tiwanaku: Papers from the 2005 Mayer Center Symposium*: 211–224. Denver: Denver Art Museum.

Williams, P.R., V. Bélisle, A. Cardona, R. Coleman, and K. Costion 2010. Obsidian as a commodity of interregional exchange in Wari sites of Southern Peru. Paper presented at the 75th Annual Meeting of the Society for American Archaeology, St. Louis.

Williams, P. Ryan, L. Dussubieux, and D.J. Nash 2012. Provenance of Peruvian Wari obsidian: comparing INAA, LA-ICP-MS, and portable XRF, in I. Liritzis and C.M. Stevenson (eds) *Obsidian and Ancient Manufactured Glasses*: 75–85. Albuquerque (NM): University of New Mexico Press.

Yataco Capcha, J. and H.G. Nami 2016. A reevaluation of Paleoamerican artifacts from Jaywamachay Rockshelter, Ayacucho Valley, Peru. *PaleoAmerica* 2(4): 368–372.

Appendix 9.1

Obsidian artifact and geologic specimen description and parts per million (ppm) elemental concentrations.
See supplementary data for this appendix online: https://doi.org/10.32028/9781803273600-online.

SAMPLE	Group	Type	weight (g)	length (mm)	width (mm)	thickness (mm)	Cortex present/ absent	K	Ca	Ti	Mn	Fe	Zn	Rb	Sr	Y	Zr	Nb	Ba	Pb	Th	U
01-00-0005	Alca-1	flake	1.4	17	23	3.5	0	37072.1	3918	753	277	5732	41.8	162.9	83.0	11.5	88.6	9.4	515.5	17.8	9.6	4.5
01-00-0007	Alca-1	flake	0.1	15	8	1	0	52470.8	3883	1094	304	6751	59.6	175.8	104.2	14.1	88.3	19.1		24.9	11.9	
01-00-0011c	Alca-1	flake	0.7	22	7	5	0	41904.4	3267	823	273	5993	43.1	151.9	88.2	12.8	96.8	11.6	328.1	17.9	10.8	4.0
01-00-0015	Alca-1	flake	0.4	13	18	3.5	0	42856.4	5269	870	228	6066	42.6	152.5	88.3	13.1	77.2	13.7		24.1	10.2	5.4
01-00-0018d	Alca-1	flake	1	20	16	4	0	38483.9	4308	760	295	5840	42.4	147.9	85.9	13.3	92.2	10.3	412.9	17.2	10.0	3.6
01-00-0019b	Alca-1	flake	1	15	14	4	0	38122.5	3923	761	289	5791	42.7	142.8	85.6	12.3	91.2	9.8	399.9	19.9	10.3	3.3
01-00-0021a	Alca-1	flake	1.4	15	25	5	0	37285.9	3858	756	269	5767	42.8	140.9	82.1	11.6	91.2	10.4	446.1	16.2	9.8	3.3
01-00-0021d	Alca-1	flake	0.3	13	16	2.5	0	46929.0	3749	909	218	6347	47.6	163.2	95.6	13.9	99.9	13.7		20.6	11.5	
01-00-0022a	Alca-1	flake	0.4	11	12	2.5	0	42548.7	4111	852	241	6075	40.5	155.3	91.5	12.7	96.1	12.4	224.8	17.2	11.2	
01-00-0031	Alca-1	flake	1	14	17	5.6	0	36965.0	5366	864	369	5697	40.0	138.1	80.2	12.0	73.1	11.2	332.9	22.5	8.5	4.7
01-00-0032a	Alca-1	flake	0.4	22	10	3	0	44469.2	3978	864	235	6205	43.1	156.0	92.4	12.6	100.1	12.5	238.7	18.6	12.1	4.8
01-00-0033a	Alca-1	flake	1.6	25	20	4.5	0	39041.6	3986	784	265	5835	41.2	145.3	85.9	12.7	91.2	11.3	359.5	19.2	11.2	
01-00-0033b	Alca-1	flake	1.5	19	32	4.5	0	38426.9	3942	769	278	5817	42.9	147.0	85.5	11.9	91.7	10.5	413.2	18.6	8.9	3.9
01-00-0034a	Alca-1	flake	0.5	13	18	3	0	41083.9	5215	833	247	5872	39.4	147.6	84.8	13.1	82.9	12.3	275.4	23.0	10.8	3.2
01-00-0036a	Alca-1	flake	2	18	21	6	0	36909.1	4555	789	241	5569	44.5	138.4	76.4	12.0	78.3	10.9	395.9	21.7	9.4	3.3
01-00-0036b	Alca-1	flake	1.5	32	18	4	0	38086.0	4519	841	211	5680	45.4	138.7	83.7	12.0	77.5	12.4	281.3	19.6	11.6	5.9
01-00-0036c	Alca-1	flake	1.6	26	18	3	0	35165.8	4902	719	279	5674	46.7	137.7	82.1	12.6	77.9	10.7	428.8	24.8	11.8	2.9
01-00-0036d	Alca-1	flake	1.2	23	16	3	0	38828.2	5185	822	226	5717	45.5	142.0	86.1	12.5	78.6	12.2	269.2	22.9	11.1	3.5
01-00-0036f	Alca-1	flake	1.3	17	16	6	0	35896.5	4330	776	287	5584	41.5	134.3	76.7	12.7	79.6	10.7	387.1	20.6	9.1	
01-00-0036g	Alca-1	flake	0.8	17	18	3.5	0	40340.9	5180	836	219	5909	40.6	148.0	83.3	11.2	78.9	13.0	299.9	24.4	10.8	4.6
01-00-0036i	Alca-1	flake	0.2	20	20	2	0	40121.5	5057	895	249	6023	42.0	146.7	88.9	11.8	87.3	12.8	249.7	23.2	10.5	5.3
01-00-0036j	Alca-1	flake	0.7	16	19	2	0	42018.6	5075	895	224	6001	45.5	152.6	89.6	12.3	80.0	14.4	232.6	21.9	9.7	5.3
01-00-0040	Alca-1	flake	0.5	9	15	5	0	37295.5	5033	835	265	5571	38.6	139.4	80.4	13.0	78.0	10.7	367.4	22.1	10.5	5.1
01-00-0041	Alca-1	flake	0.5	13	11	4	1	41222.7	5729	893	267	5925	44.1	148.9	86.5	13.1	78.2	12.6	342.8	21.0	12.2	4.8
01-00-0045	Alca-1	flake	0.5	12	13	3.5	0	38536.4	5339	835	256	5760	49.3	144.0	83.9	13.4	76.5	11.2	378.9	22.0	10.1	6.2
01-00-0055b	Alca-1	flake	0.9	15	18	3	0	37043.1	5851	778	240	5574	31.4	163.5	90.0	15.3	80.0	12.9	146.7	23.1	13.6	8.1
01-00-0060d	Alca-1	flake	0.4	15	15	2	0	44610.0	4369	915	234	6238	42.7	163.6	94.3	12.0	104.4	12.7		19.8	11.2	
01-00-0066	Alca-1	flake	0.7	18	15	3	0	38398.5	5191	812	226	5741	43.8	140.8	80.5	11.6	78.2	13.2	322.8	19.6	10.6	4.9
01-00-0071	Alca-1	flake	0.8	17	14	3.5	0	37565.7	5173	852	262	5714	39.7	139.8	84.3	11.9	82.3	11.8	297.3	20.2	11.1	5.2
01-00-0071b	Alca-1	flake	0.2	8	13	4	0	38876.2	4790	844	192	5782	39.1	141.0	82.9	11.9	77.1	12.8	260.1	22.6	10.3	4.7
01-00-0073a	Alca-1	flake	0.3	14	12	2.5	0	40407.5	5889	823	287	5832	42.0	145.2	86.8	11.7	80.8	13.1	327.7	21.7	9.2	4.1
01-00-0073d	Alca-1	flake	0.7	12	12	5.5	0	61493.4	4961	1264	368	7547	63.4	188.9	108.1	13.9	94.7	20.9		29.8	14.1	4.6
01-00-0075c	Alca-1	flake	1	21	15	3	0	41323.9	4182	803	258	5955	42.0	154.8	90.8	11.5	95.1	12.3	223.5	15.6	8.1	
01-00-0075d	Alca-1	flake	4.5	26	35	6	0	43387.2	4309	824	223	6227	40.5	162.2	95.1	12.8	95.4	12.2		17.4	9.9	

SAMPLE	Group	Type	weight (g)	length (mm)	width (mm)	thickness (mm)	Cortex present/ absent	K	Ca	Ti	Mn	Fe	Zn	Rb	Sr	Y	Zr	Nb	Ba	Pb	Th	U
01-00-0080a	Alca-1	flake	0.4	11	16	2	0	42377.4	5092	907	246	6022	43.2	151.8	90.5	12.3	85.3	15.0		22.6	12.2	4.1
01-00-0080b	Alca-1	flake	0.2	19	10	2	0	42455.3	5526	870	161	5943	40.2	153.0	89.7	11.5	83.9	14.0		20.4	9.7	4.1
01-00-0120	Alca-1	flake	0.4	16	10	2	0	42695.4	5159	886	197	6053	45.7	154.3	87.9	13.4	80.4	14.2		19.9	10.9	3.3
01-06-0001	Alca-1	flake	0.2	14	10	12.5	0	41932.7	2909	795	158	5717	40.2	147.5	86.8	12.5	90.5	11.5		15.5	8.4	
01-06-0006	Alca-1	flake	0.7	21	15	2	0	43448.3	4079	868	240	6073	43.3	156.8	93.3	13.2	101.7	11.9		16.9	9.8	
02-00-0028c	Alca-1	flake	0.4	20	17	2	0	41356.4	4099	774	246	5832	41.7	158.7	84.9	13.4	96.1	11.8	399.3	20.7	8.0	
02-00-0034d	Alca-1	flake	0.4	18	13	2	0	37673.3	3517	759	264	5716	44.7	142.0	80.8	11.7	90.9	9.6	396.4	16.8	11.7	
02-00-0037e	Alca-1	flake	0.3	10	15	1.5	0	53706.9	4029	1054	268	6963	50.7	181.1	105.9	14.9	104.8	17.6		20.1	14.3	
03-00-0001b	Alca-1	flake	1.3	17	18	8	0	40631.8	4602	773	315	6061	46.5	155.7	89.5	12.6	94.4	11.4	529.8	18.9	13.4	
03-00-0002	Alca-1	flake	0.6	16	18	3	0	40684.8	3964	796	205	5948	45.6	150.7	90.1	13.2	92.2	11.7	246.4	17.5	9.1	
03-00-0003a	Alca-1	flake	1.2	17	15	5	0	41554.5	4623	799	247	6089	42.9	153.4	89.9	13.6	92.2	12.3	240.1	19.6	10.1	
03-00-0003b	Alca-1	flake	0.3	10	12	3.5	0	36541.7	3954	730	294	5674	41.1	142.4	83.7	12.4	66.3	9.8	559.9	16.3	12.6	
03-00-0005	Alca-1	flake	0.4	12	11	4	0	39196.5	3939	782	247	5776	45.2	149.9	87.5	11.3	95.1	10.3	359.7	17.5	10.8	
03-00-0007	Alca-1	flake	1.2	16	13	7	0	36846.0	3934	708	266	5642	40.4	141.9	85.9	11.9	83.1	10.5	539.4	17.0	11.5	
03-00-0008	Alca-1	flake	0.6	12	14	4.5	0	38208.6	3796	750	233	5775	43.0	143.2	86.0	11.7	96.1	9.9	311.7	17.6	9.4	
03-00-0011c	Alca-1	flake	1.3	11	21	8	0	36188.9	4022	768	336	5677	46.9	143.8	82.9	13.4	90.8	8.2	1016.0	17.5	11.5	
03-00-0013a	Alca-1	flake	1.5	18	22	6	0	41186.7	4764	756	317	5931	44.3	153.5	90.8	15.2	99.7	10.7	443.9	17.3	12.2	
03-00-0013b	Alca-1	flake	0.1	10	7	2	0	41586.7	4368	798	258	5952	44.3	151.9	89.4	12.9	93.8	11.6	292.0	18.2	10.4	
03-00-0015	Alca-1	flake	1	15	19	6	0	38617.8	4365	750	268	5871	45.5	147.3	88.1	12.4	115.3	10.5	461.3	18.1	12.8	
03-01-0012	Alca-1	flake	0.4	13	17	2.5	0	44221.6	5277	892	269	6220	45.4	162.6	95.5	13.0	96.7	12.7		18.5	10.4	
03-04-0004a	Alca-1	flake	0.8	13	23	3	0	52694.9	4993	822	227	5998	43.1	151.3	88.2	12.1	100.8	11.8	261.0	20.4	8.5	
03-04-0004b	Alca-1	flake	0.7	17	17	3	0	57822.4	9279	801	234	6015	41.8	152.8	88.7	13.2	111.7	11.3	279.6	17.1	9.7	
03-04-0008a	Alca-1	flake	0.4	12	20	2.5	0	39450.7	3925	750	289	5935	45.2	151.7	88.4	13.2	94.2	11.5	405.5	20.1	10.5	
03-04-0008b	Alca-1	flake	0.9	24	6	5.5	0	41223.8	5555	814	223	5832	40.1	148.2	86.5	13.0	84.2	11.6	297.3	20.6	10.7	3.4
03-04-0009	Alca-1	flake	0.3	13	25	1	0	56422.9	35593	805	225	6538	43.1	173.7	100.9	12.5	108.5	15.2		19.2	12.2	
03-04-0010	Alca-1	flake	0.8	8	9	5.5	0	43527.2	6061	804	349	6243	41.6	160.2	94.4	13.9	76.6	12.1	484.9	25.3	13.8	4.0
03-04-0013	Alca-1	flake	1.3	12	15	6.5	0	34564.3	40850	931	339	6112	47.7	153.8	91.3	13.5	91.3	10.8	515.1	17.1	11.6	3.1
03-04-0016	Alca-1	flake	0.2	12	10	3	0	44459.3	4577	799	193	6094	42.5	161.7	92.4	12.4	97.5	11.3	260.5	21.0	10.0	
03-04-0020	Alca-1	flake	0.4	15	16	2.5	0	45152.7	5899	870	279	6367	46.7	166.6	95.6	14.3	98.0	12.7		22.6	12.0	
03-04-0022	Alca-1	flake	1.1	20	13	6	0	39160.5	7625	902	305	5973	47.3	148.8	86.2	12.7	94.0	10.4	472.7	16.6	12.4	
03-05-0002	Alca-1	flake	0.4	17	10	3	0	42798.5	4464	837	211	6114	44.2	159.1	92.8	12.3	106.1	12.2	241.0	18.9	10.4	
03-05-0005	Alca-1	flake	0.4	11	15	2.5	0	40610.7	11880	791	172	6067	41.6	155.6	91.0	12.8	94.7	12.1	203.5	17.3	10.5	
03-07-0007	Alca-1	flake	0.3	13	11	2.5	0	50775.8	6367	994	383	7113	55.3	183.3	106.6	11.8	116.0	14.4	287.2	20.6	12.5	
03-07-0010	Alca-1	flake	0.2	9	14	2	0	45668.7	4192	849	237	6198	46.1	163.3	99.0	12.5	103.3	14.3		17.6	11.2	
03-07-0013	Alca-1	flake	0.2	15	9	2	0	51511.1	15007	800	281	7034	54.8	185.3	106.2	14.0	103.1	15.2		19.6	11.3	
03-07-0020	Alca-1	flake	1.2	16	14	5.5	0	41587.3	4475	776	284	5866	42.8	149.2	87.8	12.0	93.4	10.4	400.4	18.2	10.0	
03-07-0021	Alca-1	flake	0.6	14	13	5	0	35745.7	4540	804	263	5750	45.2	142.0	83.1	12.0	91.4	9.3	462.3	18.4	7.7	

SAMPLE	Group	Type	weight (g)	length (mm)	width (mm)	thickness (mm)	Cortex present/ absent	K	Ca	Ti	Mn	Fe	Zn	Rb	Sr	Y	Zr	Nb	Ba	Pb	Th	U
03-07-0043	Alca-1	flake	0.4	16	12	0.4	1	42215.3	4435	810	278	6092	46.5	160.5	92.4	12.1	97.3	12.9	248.1	19.3	10.7	
03-07-0052a	Alca-1	flake	0.2	14	7	2.5	0	48410.1	4175	905	301	6433	40.8	169.7	99.2	13.6	102.2	13.3		20.1	12.2	
03-07-0052b	Alca-1	flake	0.2	12	9	2	0	52822.0	5728	975	403	6889	58.3	182.7	103.0	13.8	106.2	14.3		21.5	14.3	
03-07-0059	Alca-1	flake	0.5	15	10	4.5	0	39737.3	9351	1236	348	7147	47.8	167.2	100.0	12.9	103.1	14.2	303.7	23.1	11.8	
01-00-0004g	Alca-4	flake	0.3	22	12	1.5	0	41086.8	7126	950	268	7016	37.7	132.7	223.7	11.4	96.3	11.4		21.4	6.5	
01-00-0004h	Alca-4	flake	0.2	15	10	1.5	0	43942.4	9376	1039	322	7493	48.3	142.7	237.2	12.6	100.0	12.7		22.0	6.2	
01-10-0001	Alca-4	flake	0.2	13	10	2	0	39333.7	6809	922	237	6731	33.5	135.3	219.1	13.4	93.8	12.8		18.1	5.1	
02-00-0001a	Alca-4	flake	0.6	11	10	3	0	34693.1	7905	873	245	6262	33.7	118.6	199.0	11.0	89.8	7.9	407.4	16.8	5.7	
02-00-0001b	Alca-4	flake	0.4	10	15	3	0	35242.4	7533	837	231	6309	34.8	121.7	199.9	11.4	87.0	8.8	341.1	18.1	6.6	
02-00-0002b	Alca-4	flake	0.3	12	10	3.5	0	37965.5	7881	935	315	6802	42.5	128.8	212.4	10.7	92.7	10.6	240.7	18.1	7.9	
02-00-0006b	Alca-4	flake	1	24	12	4	0	31361.9	7320	972	311	7799	41.6	119.1	197.3	12.1	86.9	8.7	324.0	25.2	5.9	
02-00-0006e	Alca-4	flake	0.4	10	14	3	0	35945.4	8339	921	276	6500	39.7	126.3	207.8	11.3	91.1	9.8	305.6	17.3	5.3	
02-00-0007b	Alca-4	flake	0.3	15	15	2	0	37876.9	7269	934	286	6871	34.3	130.7	219.5	12.8	96.0	12.9		17.4	7.2	
02-00-0007c	Alca-4	flake	0.4	21	12	2.5	0	43275.8	7608	918	312	6961	41.8	139.3	223.7	12.0	97.0	12.4		19.5	5.7	
02-00-0008	Alca-4	flake	0.3	14	10	2	0	39822.8	8064	905	326	7566	45.6	135.0	229.3	13.1	95.5	8.5		18.2	7.5	
02-00-0009a	Alca-4	flake	1	26	20	3	0	31922.6	7121	829	343	6154	38.9	117.4	185.4	11.5	84.8	8.3	656.7	15.3	7.2	
02-00-0009c	Alca-4	flake	2.9	23	24	7	1	37948.6	8195	821	273	6562	34.2	131.5	209.7	12.1	93.3	9.8	249.0	16.9	5.3	
02-00-0009d	Alca-4	flake	0.6	20	18	2	0	37215.8	7549	929	231	7154	38.6	133.1	208.0	12.7	91.3	10.1		20.0	7.7	
02-00-0009e	Alca-4	flake	0.3	18	12	2	0	41003.7	6774	925	265	6922	37.7	137.0	217.0	14.0	95.6	10.6		19.1	5.8	
02-00-0012a	Alca-4	flake	3	19	10	2	0	36855.7	6139	828	288	6313	37.1	111.0	179.0	12.3	82.4	7.2	386.6	18.6	6.0	
02-00-0012b	Alca-4	flake	1.3	23	20	4	0	40657.5	7340	899	278	7170	37.5	137.5	223.7	12.0	98.9	13.1		21.8	5.7	
02-00-0014	Alca-4	flake	5.1	36	28	7.5	0	33043.7	6733	796	298	6311	40.6	118.5	192.4	12.4	83.5	8.2	353.1	15.8	6.2	
02-00-0017a	Alca-4	flake	0.5	14	14	3	0	39134.8	6778	869	217	6710	35.8	129.7	212.6	13.0	95.8	11.6		19.2	6.8	
02-00-0017b	Alca-4	flake	0.2	10	15	1	0	33677.1	8639	892	267	6480	37.8	124.7	201.2	11.5	89.2	8.4	354.0	21.2	7.2	
02-00-0017e	Alca-4	flake	0.3	14	10	2	0	41430.3	8213	963	274	7506	42.2	146.0	238.7	13.3	98.7	11.9		16.7	9.3	
02-00-0024a	Alca-4	flake	1.5	16	21	7	0	30711.0	7299	814	375	6187	41.0	115.1	182.0	11.0	87.0	8.2	927.2	19.1	7.9	
02-00-0024c	Alca-4	flake	1	18	20	3	0	30842.7	6097	693	259	6001	29.9	117.0	180.9	11.5	81.1	6.0	502.9	17.4	4.2	
02-00-0024d	Alca-4	flake	0.6	11	15	5	0	33277.3	6828	848	269	6560	37.0	116.3	185.5	12.4	88.0	8.2	438.7	16.0	4.6	
02-00-0028a	Alca-4	flake	0.7	16	10	4	0	36021.3	7398	902	254	6852	37.1	124.6	206.0	10.8	90.1	10.8	254.9	21.2	5.2	
02-00-0028b	Alca-4	flake	0.6	19	15	3	0	37182.4	7658	926	274	7275	41.3	133.9	221.7	15.0	94.9	10.2		18.2	6.7	
02-00-0028d	Alca-4	flake	0.4	23	9	5	0	31717.1	6351	716	255	5974	35.2	114.0	188.5	11.4	91.5	8.2	372.6	15.2	4.7	
02-00-0032a	Alca-4	flake	0.3	15	12	2.5	0	36873.6	7513	849	260	6665	39.5	129.5	206.7	13.5	90.2	8.0	234.4	20.4	3.7	
02-00-0032b	Alca-4	flake	0.3	11	17	2	0	34547.8	7760	859	266	6547	38.0	123.8	203.0	11.1	89.3	9.4	262.9	20.6	6.0	
02-00-0032c	Alca-4	flake	1	15	15	4.5	0	37420.2	7333	910	274	7384	41.4	132.9	220.3	10.2	96.1	11.7		21.7	6.1	
02-00-0032e	Alca-4	flake	0.5	18	17	2.5	0	38999.6	8179	985	335	7378	36.2	134.1	220.5	12.5	100.2	11.1		19.7	6.8	
02-00-0032f	Alca-4	flake	0.6	20	16	2.5	0	41517.1	9329	907	348	7118	44.7	142.1	230.2	13.5	98.0	12.1		19.0	8.7	
02-00-0032g	Alca-4	flake	0.4	15	18	1.5	0	33558.2	7987	935	245	6493	37.3	122.3	194.1	10.0	86.1	8.7	385.3	17.8	6.8	

SAMPLE	Group	Type	weight (g)	length (mm)	width (mm)	thickness (mm)	Cortex present/ absent	K	Ca	Ti	Mn	Fe	Zn	Rb	Sr	Y	Zr	Nb	Ba	Pb	Th	U
02-00-0032i	Alca-4	flake	0.6	15	15	3	0	39075.2	7134	875	242	6727	38.7	130.4	213.3	12.8	93.7	11.4		16.7	7.7	
02-00-0033	Alca-4	flake	0.7	13	20	3	0	33197.3	7854	938	235	7052	34.1	119.2	197.0	11.4	90.9	7.7	330.2	16.2	7.0	
02-00-0034a	Alca-4	flake	1	18	17	6.5	0	30641.5	8001	868	430	6238	41.0	115.0	190.5	11.1	85.7	8.0	1112.1	21.9	7.1	
02-00-0034b	Alca-4	flake	0.3	12	15	2	0	32923.2	7129	993	284	7050	39.5	118.1	189.6	12.1	90.2	8.9	321.5	15.4	6.3	
02-00-0034c	Alca-4	flake	7	31	20	13.5	0	60321.8	12036	958	281	8109	43.5	138.9	232.7	13.2	99.3	13.6		28.7	7.1	
02-00-0034e	Alca-4	flake	1	15	21	7	0	37935.0	7756	877	228	6823	35.6	129.2	214.7	12.1	92.9	10.2		18.1	5.0	
02-00-0034f	Alca-4	flake	0.4	19	15	2	0	35474.1	7974	944	332	6675	33.0	122.8	201.7	10.4	92.3	10.2	318.2	19.7	6.1	
02-00-0034h	Alca-4	flake	0.4	13	15	3	0	40638.0	7431	947	303	7911	40.9	140.9	219.8	13.6	98.3	13.2		18.6	6.9	
02-00-0034i	Alca-4	flake	0.2	10	14	2	0	37710.1	7098	878	254	6678	33.6	132.8	213.6	11.4	93.7	10.1		19.0	5.8	
02-00-0034l	Alca-4	flake	0.2	15	7	2.5	0	40707.4	7253	935	235	7697	47.0	138.0	223.7	13.2	99.4	13.5		21.9	5.5	
02-00-0037b	Alca-4	flake	0.2	16	8	1	0	36447.4	7988	980	276	7465	40.6	132.6	214.6	12.9	96.2	11.1		19.3	6.2	
02-00-0037c	Alca-4	flake	0.5	20	15	1.5	0	39306.7	6870	947	212	6963	37.6	132.4	213.1	12.9	92.3	12.2		17.3	8.9	
02-00-0037d	Alca-4	flake	0.5	16	13	2	0	33930.9	8224	822	290	6552	34.6	119.9	209.5	12.8	88.8	8.5	400.7	14.6	7.2	
02-00-0037f	Alca-4	flake	0.2	7	17	1.5	0	36360.5	7801	1010	256	7623	31.8	132.1	212.2	11.6	91.8	10.6		16.7	5.4	
02-00-0037h	Alca-4	flake	0.6	15	15	4	0	37124.8	8281	1028	296	7758	39.6	134.4	219.1	11.4	97.0	10.3		22.8	7.8	
02-00-0037i	Alca-4	flake	0.3	17	11	1	0	45079.3	11865	1035	335	7247	38.0	141.4	235.1	14.5	100.6	12.0		18.7	6.4	
02-00-0037j	Alca-4	flake	0.6	10	14	4.5	0	41868.8	6462	936	362	7211	39.5	143.3	230.2	11.7	99.3	11.1		18.1	5.6	
02-00-0038	Alca-4	flake	0.4	17	15	2	0	34082.4	7413	955	258	7325	33.8	122.2	198.6	10.6	91.7	9.5	258.1	17.6	5.4	
02-00-0038b	Alca-4	flake	0.3	10	14	2.5	0	40726.9	7627	900	282	6867	36.9	134.0	223.5	11.9	94.1	10.4		18.4	5.6	
02-00-0039a	Alca-4	flake	0.3	15	15	2	0	31129.6	7236	871	333	6548	35.9	113.6	187.7	11.7	83.0	7.7	733.4	20.7	6.9	
02-00-0039b	Alca-4	flake	0.6	15	15	3.5	0	31404.7	7356	880	358	6541	40.7	113.2	185.3	11.9	85.0	9.4	749.6	18.6	7.7	
02-00-0039c	Alca-4	flake	0.3	16	15	2.5	0	37408.0	7551	914	307	7103	42.3	129.0	215.9	13.6	94.5	10.5		18.2	7.9	
02-00-0039d	Alca-4	flake	0.3	13	13	2	0	39446.6	7628	841	272	6827	39.4	133.1	221.3	13.4	96.2	11.0		18.4	7.5	
02-00-0039e	Alca-4	flake	0.3	15	15	2.5	0	32930.6	7768	885	287	6432	38.6	117.9	194.0	11.2	88.6	9.1	382.1	18.4	7.9	
02-00-0039g	Alca-4	flake	3.3	27	20	9.5	0	34593.9	7646	841	234	6563	36.4	121.0	199.8	11.1	88.5	8.7	256.6	12.2	5.4	
02-00-0039h	Alca-4	flake	0.6	16	19	1.5	0	42672.7	12662	881	328	7317	41.5	141.6	226.4	13.5	98.6	12.8		17.5	8.7	
02-00-0039i	Alca-4	flake	0.7	23	21	2	0	30953.4	7953	950	321	7054	29.5	116.5	197.5	12.9	88.9	8.5	384.6	23.2	6.6	
02-00-0039j	Alca-4	flake	0.7	17	27	3	0	35730.4	8346	1046	231	10813	39.3	130.2	215.4	12.4	94.1	9.1		20.5	5.5	
02-00-0039k	Alca-4	flake	0.7	23	14	2.5	0	35194.0	6230	877	322	6364	33.8	125.2	170.5	11.2	85.1	9.7	244.2	13.7	4.9	
02-00-0039l	Alca-4	flake	1	14	23	3	0	33660.8	8341	1003	423	6621	41.4	119.3	196.3	12.1	88.5	9.1	795.1	21.9	9.5	
02-00-0039m	Alca-4	flake	1	18	15	6	0	38045.4	11892	969	246	10739	41.0	136.6	231.0	13.3	95.3	12.3		21.8	6.4	
02-00-0039n	Alca-4	flake	0.5	19	13	6	0	34956.2	7005	827	222	6429	32.9	122.1	195.5	11.1	89.6	9.1	258.1	14.8	5.9	
02-00-0039p	Alca-4	flake	0.3	15	15	2	0	40114.6	8298	976	268	7044	39.2	138.2	225.3	12.7	97.1	12.1		20.0	7.9	
02-00-0039q	Alca-4	flake	0.5	21	15	3	0	40693.2	8011	948	279	6976	33.5	137.8	224.0	12.3	98.1	11.7		22.1	7.5	
02-00-0039r	Alca-4	flake	0.4	23	20	2	0	41526.4	7335	966	259	7084	36.0	138.3	230.5	11.6	97.1	12.3		20.1	5.9	
02-00-0041a	Alca-4	flake	0.4	15	13	1.5	0	29901.9	6106	776	261	6767	39.8	112.2	182.2	10.6	84.8	6.0	541.6	20.4	5.0	
02-00-0041b	Alca-4	flake	0.9	16	15	3	0	32931.8	8205	1014	301	7698	38.6	121.9	202.3	10.8	89.3	6.9	312.7	25.8	8.5	

SAMPLE	Group	Type	weight (g)	length (mm)	width (mm)	thickness (mm)	Cortex present/ absent	K	Ca	Ti	Mn	Fe	Zn	Rb	Sr	Y	Zr	Nb	Ba	Pb	Th	U
02-00-0041c	Alca-4	flake	1.1	18	18	6	0	31272.3	7665	982	332	7956	39.2	116.7	187.7	12.6	88.5	7.4	427.5	22.7	6.7	
02-00-0041d	Alca-4	flake	0.7	14	20	2.5	0	31293.2	8336	992	301	6786	35.6	126.3	204.5	12.8	92.7	8.5	415.0	18.8	7.1	
02-00-0041e	Alca-4	flake	1.1	22	14	5.5	0	37327.6	7877	1026	250	10667	39.4	134.3	226.0	13.7	94.2	10.7		20.1	7.7	
02-04-0002	Alca-4	flake	0.1	10	10	1	0	53335.9	14115	1194	463	8049	42.4	162.6	271.0	14.6	110.7	16.9		23.3	6.5	
02-04-0003b	Alca-4	flake	0.2	10	13	2.5	0	33242.7	62462	909	232	7000	39.8	137.4	216.6	11.9	94.0	13.3		18.9	6.3	
02-07-0009	Alca-4	flake	0.2	13	11	2	0	38676.2	8268	968	301	7021	40.8	135.1	222.7	12.6	93.8	11.1		15.4	6.2	
02-07-0010	Alca-4	flake	0.2	11	15	1	0	40289.2	7277	922	278	7863	43.0	138.7	225.1	10.9	98.0	12.0		21.9	7.0	
02-07-0016a	Alca-4	flake	0.1	9	14	1	0	47860.6	15047	845	294	5180	50.5	153.3	248.7	14.0	106.5	12.5		23.2	11.0	2.7
02-07-0016b	Alca-4	flake	0.1	10	10	1.5	0	44659.8	32152	758	394	4972	51.9	154.2	248.0	14.9	104.6	14.7		22.5	10.7	
02-07-0020	Alca-4	flake	0.3	22	9	3	0	36619.3	7904	963	285	6465	38.2	129.0	172.8	11.8	81.0	12.8		21.2	6.1	
03-00-0009	Alca-4	flake	0.5	10	15	4	0	35240.4	7931	817	297	6333	31.7	122.0	196.4	11.6	91.2	9.6	369.5	18.3	6.3	
03-07-0009	Alca-4	flake	0.8	24	10	3.5	1	34671.7	7146	779	271	6267	34.2	118.3	194.6	11.1	88.4	8.2	357.9	15.4	7.6	
03-07-0040	Alca-4	flake	0.2	10	13	2.5	0	33902.8	6192	795	130	6106	34.2	118.1	190.4	10.9	87.0	8.0	287.6	14.0	3.8	
01-00-0063a	Anillo	flake	5.5	31	21	10	1	37133.1	7488	856	297	6137	40.7	166.0	154.8	13.5	92.2	13.6	434.9	24.2	17.2	
01-00-0063b	Anillo	flake	1.7	20	15	8	0	42231.1	8113	850	356	6113	34.5	168.4	157.9	13.6	99.1	15.2	412.1	27.4	15.9	5.0
01-00-0063c	Anillo	flake	1	19	17	4	0	38180.7	8355	923	338	6358	41.2	171.3	163.1	13.7	96.1	13.6	404.1	25.5	19.5	4.9
01-00-0075a	Anillo	flake	0.6	18	15	2.5	0	38078.6	7223	830	429	6608	50.3	176.2	172.2	13.5	110.7	12.5	712.3	22.1	16.2	5.7
01-00-0075b	Anillo	flake	0.6	18	21	2.5	0	39200.7	6201	850	245	6249	36.7	172.0	167.5	14.2	105.4	13.9	318.9	21.9	18.1	4.5
01-00-0122	Anillo	flake	0.7	21	15	2	0	35816.5	7452	759	299	5858	39.1	160.3	150.7	14.6	93.3	12.6	422.5	26.2	14.8	5.6
01-10-0010	Anillo	flake	1.7	15	22	8	1	40443.1	7150	888	314	3161	42.0	179.5	165.1	12.9	113.8	5.0	683.9	23.3	17.2	4.7
02-00-0029a	Anillo	flake	2.5	23	20	6.5	0	36838.4	6253	823	357	6280	39.6	169.6	163.0	13.8	111.0	12.2	719.9	20.2	20.5	5.0
02-06-0005	Lisahuacho	flake	0.3	14	12	2	0	42717.5	10588	1212	230	7561	42.8	153.1	242.6	11.3	138.1	9.4		18.1	17.5	2.7
01-00-0008	Quispisisa	flake	1.7	26	15	6	1	38369.1	7073	821	114	5675	30.9	171.3	126.8	9.5	74.4	10.2	212.3	25.1	17.2	10.0
01-00-0034b	Quispisisa	flake	0.3	12	18	2.5	0	41564.3	7096	865	73	5829	29.6	182.2	136.4	10.8	78.4	12.6		27.8	15.3	7.4
01-00-0039	Quispisisa	flake	0.5	13	15	3	0	42520.9	8803	950	125	6177	33.1	191.6	147.2	12.1	81.5	12.9		29.0	17.9	10.6
01-00-0057a	Quispisisa	flake	0.3	10	17	2	0	45988.8	7838	1041	107	6450	30.4	205.5	155.8	11.0	84.8	15.9		31.2	20.1	9.7
01-00-0057b	Quispisisa	flake	0.3	10	16	2.5	0	40517.1	7022	909	165	5963	27.7	183.3	139.4	9.6	80.6	12.6		27.2	16.0	9.7
02-00-0004	Quispisisa	flake	0.3	10	13	2.5	0	43096.5	6455	869	117	6227	30.4	197.2	152.1	11.9	75.9	11.6		26.2	16.6	5.6
02-00-0006c	Quispisisa	flake	0.5	20	19	1	0	48931.5	6639	932	122	6846	29.7	223.1	169.2	10.5	106.1	14.3		29.4	18.8	7.9
02-00-0006d	Quispisisa	flake	0.4	14	15	1	0	52496.9	6274	846	123	7116	34.4	230.9	171.7	12.6	80.5	17.1		30.4	23.0	
02-00-0017c	Quispisisa	flake	0.5	18	17	2	0	42798.8	6169	897	134	6340	29.1	195.8	150.0	11.6	75.1	12.0		23.5	19.7	
02-00-0017d	Quispisisa	flake	0.7	15	17	3	0	53291.6	6005	1090	122	7192	35.9	236.5	180.4	12.3	109.9	18.8		31.0	23.0	4.9
02-03-0001	Quispisisa	flake	0.3	15	8	3	0	39237.0	5306	736	100	5992	30.5	190.2	142.0	10.3	73.2	12.0	136.6	22.0	18.1	8.5
02-07-0019	Quispisisa	flake	0.4	11	19	2.5	0	25388.9	111669	1035	75	6675	38.5	186.5	146.1	12.9	91.1	10.6		22.5	14.7	4.2
01-00-0017a	Alca-1	flake	0.8	18	15	3	0	39033.9	3701	782	209	5783	42.2	148.6	85.3	11.7	94.7	10.5	308.5	18.6	10.3	3.3
01-00-0018e	Alca-1	flake	0.6	17	13	2.5	0	41791.3	4116	829	242	6048	41.8	157.4	90.0	12.4	99.5	12.3	277.1	18.8	11.3	
01-00-0055a	Alca-1	flake	1.6	20	20	5	0	38683.3	6413	804	322	5695	32.5	166.6	91.7	14.5	82.5	13.4	232.8	25.2	16.0	11.4

SAMPLE	Group	Type	weight (g)	length (mm)	width (mm)	thickness (mm)	Cortex present/ absent	K	Ca	Ti	Mn	Fe	Zn	Rb	Sr	Y	Zr	Nb	Ba	Pb	Th	U
01-00-0061	Alca-1	flake	4.7	26	23	7.5	0	36315.3	5323	807	371	5634	40.8	137.1	80.1	11.2	73.5	11.5	625.2	20.3	10.7	5.8
01-00-0070	Alca-1	flake	1	20	26	2	0	41121.7	5010	879	231	5850	44.3	148.6	85.4	12.6	85.4	12.2		20.5	10.9	4.0
01-10-0002	Alca-1	flake	1	17	16	3.5	0	38779.3	11910	957	222	5930	38.8	149.8	89.4	12.5	92.7	9.3	312.4	18.0	10.5	
01-10-0008	Alca-1	flake	2.8	34	18	5	0	39690.7	4047	769	260	5819	39.2	146.5	86.3	12.1	94.6	10.4	335.3	17.7	8.7	
03-01-0009	Alca-1	flake	0.4	14	10	3.5	0	40796.6	5781	810	264	6160	43.8	152.7	91.3	12.7	97.3	10.6	300.7	17.6	10.4	
03-04-0012	Alca-1	flake	1.2	13	16	6	0	38792.1	4473	812	297	5755	41.5	145.9	85.2	10.4	92.0	10.7	547.3	16.0	10.8	3.3
03-05-0015	Alca-1	flake	1	20	14	4	0	41394.9	4241	791	243	5946	44.9	151.3	88.6	12.2	96.0	10.4	302.6	18.0	12.5	
03-05-0017	Alca-1	flake	1	16	18	4	0	40862.1	5384	894	293	5849	39.2	152.0	87.8	12.8	95.5	10.3	353.4	16.0	11.6	
03-05-0018	Alca-1	flake	2.3	32	23	3	0	34750.9	4870	802	272	5855	42.0	143.7	83.4	12.3	93.1	10.1	346.2	18.1	9.6	
03-06-0001b	Alca-1	flake	0.5	11	14	4	0	42076.4	4535	788	249	6059	45.3	154.8	90.3	13.0	104.1	11.5	291.3	16.5	12.2	
03-07-0014	Alca-1	flake	0.6	10	15	5	0	35149.5	3975	789	312	6232	47.5	151.0	87.8	13.3	92.2	10.6	558.8	18.1	10.5	
01-00-0027	Anillo	flake	1	17	16	3.5	0	39054.3	7732	837	297	6056	39.7	170.0	161.7	14.6	95.8	13.6	340.1	26.9	17.8	
01-00-0014	Alca-1	flake - bifacial thinning flake	0.2	13	15	1.5	0	52561.6	6023	1098	334	6889	49.0	175.1	104.4	14.7	94.3	18.2		27.3	14.3	7.3
01-00-0026a	Alca-1	flake - bifacial thinning flake	0.3	15	11	2	0	50420.8	4012	936	276	6674	47.0	171.5	103.2	14.1	106.3	15.1		20.5	12.3	3.2
01-00-0036e	Alca-1	flake - bifacial thinning flake	0.6	15	17	2	0	39178.5	4376	865	181	5872	42.6	145.2	82.5	12.9	80.5	11.3		21.7	9.9	3.0
01-00-0050	Alca-1	flake - bifacial thinning flake	0.3	15	10	2.5	0	44333.1	5251	901	240	6171	38.0	155.1	92.6	13.5	81.6	15.4		24.2	10.6	4.0
01-00-0051a	Alca-1	flake - bifacial thinning flake	0.6	12	22	3	0	42056.6	4610	823	185	6026	37.1	182.6	99.1	14.4	98.8	12.8		15.5	16.2	
01-00-0060c	Alca-1	flake - bifacial thinning flake	0.6	14	15	3	0	39261.6	3823	751	195	5947	38.1	152.2	89.3	12.9	93.4	11.2	279.0	17.3	11.2	
01-19-0001	Alca-1	flake - bifacial thinning flake	0.5	17	18	1.5	0	46453.7	5124	949	228	6236	44.4	162.8	97.4	12.7	88.6	16.1		21.7	12.8	3.4
03-05-0014	Alca-1	flake - bifacial thinning flake	0.6	15	13	2	0	42262.6	4517	796	226	5989	44.1	156.2	91.0	14.2	97.5	11.0	273.9	20.4	11.1	
02-00-0002a	Alca-4	flake - bifacial thinning flake	0.7	19	20	2	0	3702.7	643	204	303	6445	43.1	125.6	204.2	12.5	90.7	8.9	222.7	19.0	6.1	
02-00-0011	Alca-4	flake - bifacial thinning flake	1.2	27	20	2.5	0	35505.7	7846	841	237	6402	36.8	123.0	201.6	11.8	89.5	10.1	288.1	16.8	6.2	
01-00-0030	Jampatilla	flake - bifacial thinning flake	0.9	10	20	4.5	0	36783.6	11999	1051	416	7731	51.5	145.9	290.5	26.0	159.5	16.5	272.2	30.2	9.4	6.6

SAMPLE	Group	Type	weight (g)	length (mm)	width (mm)	thickness (mm)	Cortex present/ absent	K	Ca	Ti	Mn	Fe	Zn	Rb	Sr	Y	Zr	Nb	Ba	Pb	Th	U
02-07-0022	Quispisisa	flake - bifacial thinning flake	0.4	13	18	2	0	40147.3	7644	839	97	6158	27.4	190.4	144.6	11.6	71.5	12.0		22.8	18.3	4.6
01-00-0002	Alca-1	shatter	1.2	12	15	6	1	36271.7	5317	789	278	5588	41.6	137.0	80.1	12.0	74.8	12.7	437.0	24.0	9.9	4.8
01-00-0021b	Alca-1	shatter	1.5	16	19	6	0	38313.4	4002	764	336	5801	41.9	143.1	85.3	11.9	95.0	9.5	540.7	17.9	11.4	3.7
01-00-0042	Alca-1	shatter	0.5	11	11	4	0	37182.3	5453	819	291	5667	41.2	141.8	80.8	13.0	80.4	12.5	376.4	21.9	10.6	3.5
01-00-0048e	Alca-1	shatter	0.3	10	15	2.5	0	40636.3	5165	880	214	5842	41.7	147.9	87.1	11.5	84.2	12.6	251.6	22.3	11.7	3.2
01-00-0049	Alca-1	shatter	0.4	10	12	5	0	34514.1	4381	717	200	5464	38.6	133.6	77.0	11.6	80.2	12.0	433.4	19.5	9.8	
01-00-0073c	Alca-1	shatter	0.5	13	15	3	0	40807.2	4807	886	219	5813	37.4	148.4	83.0	12.1	77.1	14.0		20.3	10.5	4.6
01-05-0003	Alca-1	shatter	1.2	20	16	5	0	37569.4	6462	783	247	5576	31.3	163.8	88.1	13.7	80.6	14.2	233.9	23.1	13.8	5.5
01-06-0002	Alca-1	shatter	0.5	16	11	19	0	43444.7	4593	1004	242	6221	44.9	163.6	91.4	12.1	99.9	10.5	251.1	17.5	11.8	3.6
01-10-0004	Alca-1	shatter	1.2	11	16	5.5	0	39363.8	4941	770	376	5922	44.0	150.8	87.8	12.5	94.6	10.4	751.6	21.2	12.4	3.3
03-00-0001a	Alca-1	shatter	2.7	15	20	10.5	0	37895.9	3379	673	438	5595	47.4	137.9	75.5	11.7	87.6	10.0	948.0	17.6	11.6	
03-00-0011a	Alca-1	shatter	2.2	15	30	5	0	48256.1	4599	775	332	5990	47.2	150.7	85.0	14.5	99.1	11.0	501.7	18.1	10.3	
03-00-0011b	Alca-1	shatter	1.1	14	21	8.5	0	54066.2	4230	768	287	6000	44.9	155.0	90.2	13.2	93.5	11.9	335.9	19.0	12.2	
03-00-0011d	Alca-1	shatter	1.1	10	19	7.5	0	35075.8	4037	690	395	5780	46.3	145.6	87.2	12.9	94.5	11.4	1060.0	20.6	12.5	
03-03-0001	Alca-1	shatter	1	13	24	6	0	33243.9	5881	886	365	5961	49.2	140.3	82.5	11.4	93.5	9.6	578.3	19.3	11.4	
03-04-0003	Alca-1	shatter	1	13	17	7.5	0	43653.7	6071	779	398	6243	47.6	161.0	94.0	13.0	98.6	12.9	643.0	20.4	13.6	
03-04-0021	Alca-1	shatter	0.5	7	15	4	0	40915.0	6965	796	287	6020	45.3	155.1	90.6	13.5	73.1	11.0	378.1	20.2	13.0	2.7
03-05-0003	Alca-1	shatter	0.9	12	20	4	0	39735.4	4471	754	299	5811	43.5	148.6	85.8	13.9	101.2	11.1	346.8	16.5	9.9	
03-05-0010	Alca-1	shatter	0.3	17	6	3.5	0	48297.8	4478	923	260	6387	45.2	173.3	101.7	15.4	100.7	14.2		20.2	12.9	
03-05-0016	Alca-1	shatter	0.2	11	7	2	0	49575.0	3178	902	342	6897	51.5	177.4	102.9	13.1	110.2	14.1	212.0	21.9	14.9	
03-06-0003	Alca-1	shatter	1.7	22	22	7	0	52110.7	4385	777	270	5706	42.9	143.8	84.5	13.5	91.7	9.7	539.3	17.8	9.4	2.8
03-07-0039	Alca-1	shatter	0.3	11	8	4	0	42206.6	3387	818	236	5787	40.3	148.7	85.9	11.3	86.5	11.3	320.9	16.1	10.7	
01-00-0004a	Alca-4	shatter	1	20	11	4	0	32498.5	7348	840	283	6330	40.0	117.1	191.0	12.0	85.1	7.9	417.1	19.1	5.1	
01-00-0004b	Alca-4	shatter	1.2	20	12	7.5	0	30684.6	6714	787	351	6280	35.8	116.4	184.2	11.2	85.4	7.4	674.7	17.9	6.6	3.0
01-00-0004c	Alca-4	shatter	1.4	19	12	6	0	32938.0	7588	764	375	6233	39.4	114.1	191.2	11.7	87.7	8.1	718.5	19.0	6.4	
01-00-0004d	Alca-4	shatter	1.2	12	16	5.5	0	32491.6	7268	770	362	6194	38.6	115.2	190.0	11.5	85.9	7.7	745.8	17.5	7.4	
01-00-0004e	Alca-4	shatter	1.3	19	10	8.5	0	31719.6	7141	862	378	6473	39.0	116.1	186.9	10.7	84.9	7.7	774.3	18.0	6.9	
01-00-0004f	Alca-4	shatter	0.4	15	12	2	0	41126.7	6824	916	271	6997	37.5	132.9	223.6	12.5	94.8	11.9		19.5	6.8	
01-00-0004i	Alca-4	shatter	0.4	13	8	4	0	38837.5	9482	1031	414	7260	44.6	116.3	226.9	12.1	96.6	9.9	425.0	20.8	8.2	
02-00-0009b	Alca-4	shatter	4.5	38	18	8	0	40648.3	7225	870	316	6376	39.4	116.7	188.8	11.6	84.2	7.7	444.9	21.7	6.0	
02-00-0024b	Alca-4	shatter	2.5	15	23	7	0	33738.5	9049	1202	392	7514	39.9	124.6	208.6	13.7	93.4	10.1	379.2	20.5	7.7	
02-00-0034g	Alca-4	shatter	0.5	14	12	4	0	34778.1	7689	949	283	7109	36.3	127.8	214.6	10.9	92.3	12.1	282.2	18.4	5.9	
02-00-0039f	Alca-4	shatter	6.4	17	21	11.5	0	33979.4	7305	962	262	7238	36.4	125.3	204.9	12.7	92.4	10.9		23.2	7.9	
02-00-0039o	Alca-4	shatter	1.4	15	15	8.5	0	37602.4	6705	900	224	6552	38.5	127.9	214.3	12.5	92.6	10.9		17.2	5.0	
02-07-0014	Alca-4	shatter	0.8	10	22	3	0	35138.7	9171	1076	306	6932	37.2	124.4	204.4	10.4	90.9	9.1	301.4	16.7	5.3	
03-07-0002	Alca-4	shatter	0.4	8	15	4	0	36124.7	7438	866	272	6473	38.2	125.8	205.3	12.0	88.6	8.7	318.4	17.1	6.0	

SAMPLE	Group	Type	weight (g)	length (mm)	width (mm)	thickness (mm)	Cortex present/ absent	K	Ca	Ti	Mn	Fe	Zn	Rb	Sr	Y	Zr	Nb	Ba	Pb	Th	U
02-03-0002	Quispisisa	shatter	0.2	8	14	3	0	46830.1	6765	904	144	6490	33.5	213.2	161.6	12.8	81.8	12.4		23.2	17.5	6.2
9003.1.3	Geologic Quispisisa							36265.9	6477	883	177	5753	34.5	177.1	134.9	10.7	90.7	2.9	485.5	28.7	18.2	5.3
9003.2.2	Geologic Quispisisa							37767.6	7093	919	321	5769	34.7	182.2	139.3	11.7	91.7	3.9	672.8	24.0	18.7	7.3
9004.2.3	Geologic Quispisisa							36025.7	6566	849	307	5564	32.5	179.4	135.6	10.7	88.0	1.0	701.5	24.5	19.9	6.4
9004.3.4	Geologic Quispisisa							36701.9	6531	897	281	5647	31.2	181.5	136.2	10.2	87.3	3.3	625.8	24.3	18.5	5.9
9006.1.5	Geologic Quispisisa							37274.5	6799	912	295	5731	31.9	178.6	136.2	10.2	85.0	3.4	761.3	23.8	20.2	7.1
9006.2.2	Geologic Quispisisa							38002.8	6580	864	269	5244	30.7	190.3	138.9	14.2	91.0	2.8	721.9	27.0	19.0	11.0
9006.3.2	Geologic Quispisisa							37726.2	7092	942	320	5540	33.0	183.9	140.5	11.8	89.0	3.8	748.0	27.2	20.3	7.1
9006.4.3	Geologic Quispisisa							37235.3	6497	903	264	5500	32.0	183.0	139.6	11.0	87.5	3.2	504.0	24.5	16.5	6.5
9006.5.2	Geologic Quispisisa							35823.8	5879	793	185	5351	27.9	179.2	136.0	11.3	84.9	3.7	529.3	22.1	17.7	6.9
9007.2.4	Geologic Quispisisa							37326.6	6897	903	210	5631	35.0	185.2	139.8	11.6	88.4	3.7	531.0	24.4	17.7	6.8
9029.2.2	Geologic Quispisisa							36594.3	6225	811	171	5428	28.4	186.1	137.0	9.6	88.7	3.1		26.5	15.8	5.8
9029.5.2	Geologic Quispisisa							35331.2	5324	755	296	5415	34.0	173.3	134.2	11.8	85.6	1.9	754.6	21.9	18.6	6.0
9031a.3.3	Geologic Quispisisa							35175.0	5679	776	339	5910	31.9	176.0	132.5	11.6	86.8	3.4	811.0	22.8	19.1	7.8
9031a.5.3	Geologic Quispisisa							35710.8	6382	1031	221	5438	33.8	177.8	133.9	11.1	85.4	3.6	556.9	24.8	19.6	7.4
9031a.7.3	Geologic Quispisisa							37463.2	7088	899	232	5304	30.3	187.4	137.0	10.5	87.4	3.9	642.3	29.2	18.1	7.0
9087.1.3	Geologic Quispisisa							33863.7	5673	774	201	5494	27.5	169.2	131.4	11.2	86.5	2.0	667.9	25.8	16.9	5.7
9005.1.2	Geologic Quispisisa							36788.3	6607	881	282	5679	35.7	181.7	137.1	11.2	88.6	2.8	778.7	26.1	17.1	7.2
9007.3.4	Geologic Quispisisa							37275.1	6781	887	347	5723	41.7	187.5	139.2	9.7	90.5	3.2	666.9	24.8	17.9	8.5
QSS001	Geologic Quispisisa							34547.1	4944	746	269	5826	32.7	175.3	132.9	11.3	73.9	9.2	733.7	23.7	15.7	8.2
Alca1-KRA-001	Geologic Alca-1							36978.5	3756	723	422	5751	47.4	139.1	81.9	12.4	90.4	9.9	1019.7	17.1	12.5	5.1
Alca1-KRA-026	Geologic Alca-1							36572.4	4268	800	421	5907	53.8	143.0	83.4	13.1	89.5	9.8	934.9	19.1	11.1	4.4
ALCA1-kra061	Geologic Alca-1							36812.2	5364	842	452	2793	44.6	143.1	84.0	11.2	85.9	4.0	1043.6	19.7	12.3	3.8
Alca1-KRA-065	Geologic Alca-1							37810.6	4095	743	406	5811	49.3	145.3	83.2	13.3	93.5	10.5	993.2	19.1	11.2	4.4
Alca1-KRA-070	Geologic Alca-1							36016.6	3990	743	468	5754	47.1	143.9	83.2	12.4	90.5	10.4	983.8	18.7	10.8	5.6
Alca1-KRA-095	Geologic Alca-1							37288.4	4154	763	440	5795	46.3	143.4	83.4	12.8	84.0	10.2	973.0	19.0	12.3	5.5

SAMPLE	Group	Type	weight (g)	length (mm)	width (mm)	thickness (mm)	Cortex present/ absent	K	Ca	Ti	Mn	Fe	Zn	Rb	Sr	Y	Zr	Nb	Ba	Pb	Th	U
ALCA1-KRA113	Geologic Alca-1							36924.8	4282	791	477	2725	45.1	138.1	85.7	12.8	96.2	3.4	1081.3	21.6	13.3	5.5
Alca1-M25	Geologic Alca-1							37119.6	4051	748	420	5802	50.6	145.0	82.5	12.4	89.6	10.0	966.2	20.4	11.7	5.4
ALCA1-m94	Geologic Alca-1							36393.6	5407	865	368	2774	45.8	140.7	87.4	12.9	95.7	3.1	976.1	22.4	11.4	3.2
Alca2-KRA-003	Geologic Alca-2							35616.6	5676	1167	420	7196	51.1	147.5	153.8	13.7	151.0	10.7	944.1	17.1	15.3	5.3
Alca2-KRA-004	Geologic Alca-2							35654.7	5355	1085	429	6754	49.4	149.2	150.8	13.7	146.0	10.3	978.4	21.5	15.1	5.3
Alca2-KRA-151	Geologic Alca-2							36978.0	5480	1099	425	6660	51.8	150.1	149.0	13.0	148.8	11.2	1006.7	20.2	14.7	5.2
Alca3-KRA-010	Geologic Alca-3							35414.6	7873	1219	554	7246	53.6	134.0	233.5	14.8	147.1	9.7	1029.3	19.0	12.2	3.7
Alca3-KRA-011	Geologic Alca-3							34989.4	7839	1179	515	7341	54.2	133.0	229.1	14.1	148.1	9.5	997.5	21.8	11.9	5.0
Alca3-KRA-012	Geologic Alca-3							33786.4	8201	1169	516	7215	53.7	133.7	232.7	14.1	147.0	9.8	995.7	20.0	10.9	4.9
Alca3-KRA-013	Geologic Alca-3							34144.6	7938	1172	543	7163	51.8	133.3	232.0	13.7	156.5	9.1	1075.0	20.0	10.4	4.9
Alca3-KRA-094	Geologic Alca-3							33531.1	7924	1190	528	7256	54.1	136.3	230.3	14.2	146.0	9.8	1047.9	20.1	11.6	4.3
Alca3-KRA-161	Geologic Alca-3							33305.1	7772	1163	455	7130	47.9	134.5	231.7	13.8	147.5	9.4	864.4	19.1	11.3	4.9
Alca3-KRA-162	Geologic Alca-3							33420.2	7936	1181	506	7218	56.2	134.2	234.7	14.6	146.8	10.5	1021.2	18.7	12.6	4.8
Alca3-KRA-164	Geologic Alca-3							33449.2	8410	1208	509	7268	53.5	134.2	231.8	13.9	146.8	9.7	990.4	27.3	11.1	5.4
Alca4-KRA-097	Geologic Alca-4							29172.9	6621	963	522	6483	46.5	115.7	163.8	11.5	89.0	8.2	1067.1	26.5	5.1	
Alca4-KRA-098	Geologic Alca-4							30634.0	6377	790	519	6144	45.5	114.3	160.7	11.6	83.4	7.7	1040.1	22.5	5.5	4.5
ALCA4-kra099	Geologic Alca-4							31485.4	6832	860	437	3446	46.5	108.0	169.9	12.8	87.8	0.6	1160.9	19.9	8.1	4.1
Alca4-KRA-100	Geologic Alca-4							30649.7	6545	837	493	6168	45.6	112.6	161.4	12.3	87.0	8.0	1053.7	23.9	6.5	3.6
ALCA4-kra242(1)	Geologic Alca-4							30846.6	7035	802	426	3079	41.1	109.6	169.2	11.4	85.7	1.2	1019.3	17.7	7.0	3.0
ALCA4-kra242(2)	Geologic Alca-4							31072.4	6995	793	544	2894	35.3	111.0	169.8	11.9	83.5	-0.6	1126.1	18.3	8.8	4.3
Alca4-KRA-252	Geologic Alca-4							30341.3	6648	856	506	6021	45.4	114.8	155.9	11.5	85.9	8.5	1049.5	24.0	5.4	4.0
ALCA4-KRA-254	Geologic Alca-4							30088.0	6191	839	507	6055	45.0	116.0	159.8	11.8	88.1	8.1	1016.8	18.4	6.9	3.3
Alca4-KRA-257	Geologic Alca-4							29657.8	6596	858	510	6124	43.9	113.9	160.6	12.1	86.7	7.6	1042.2	23.7	6.2	4.2
ALCA5-KRA-107	Geologic Alca-5							34009.1	4549	750	427	5693	42.2	133.3	116.7	11.1	58.1	10.1	825.1	18.3	9.2	5.1
ALCA5-KRA-108	Geologic Alca-5							35677.6	5033	804	465	5811	48.3	136.8	119.2	13.2	62.6	9.7	996.2	20.1	12.7	4.6
ALCA5-KRA-109	Geologic Alca-5							35984.9	5128	768	351	5782	41.3	136.3	121.6	11.5	73.2	9.1	599.2	17.6	10.2	3.3
ALCA5-KRA-110	Geologic Alca-5							34626.1	4764	735	317	5666	42.2	133.9	119.2	11.6	74.1	9.8	446.9	15.9	10.4	4.0
ALCA5-KRA-111	Geologic Alca-5							34718.0	4895	761	465	5810	44.1	135.2	120.1	12.6	69.0	10.5	991.4	20.9	11.7	5.0
ALCA5-KRA-112	Geologic Alca-5							36215.9	5131	798	461	5832	46.5	136.7	119.3	13.5	66.3	9.9	910.8	18.6	10.9	4.0
ALCA7-KRA-101	Geologic Alca-7							34490.1	6354	751	422	5706	37.3	159.1	147.6	13.0	58.0	10.9	817.7	23.4	15.2	5.7
ALCA7-KRA-102	Geologic Alca-7							35541.9	6799	735	437	5747	34.0	161.5	147.0	13.7	58.8	10.1	837.1	23.5	13.8	4.7
ALCA7-KRA-189	Geologic Alca-7							35447.2	6382	722	444	5711	34.9	162.0	147.8	13.5	59.2	11.1	758.2	21.4	14.8	5.8
ALCA7-KRA-195	Geologic Alca-7							34764.9	6572	751	434	5790	35.8	159.6	146.1	13.8	60.5	11.0	768.1	24.6	15.4	5.7
ALCA7-KRA-197	Geologic Alca-7							34966.6	6298	761	374	5732	31.0	162.6	144.5	13.1	57.6	10.1	701.5	20.8	14.5	5.3
ALCA7-KRA-198	Geologic Alca-7							35297.5	6454	735	377	5691	33.5	160.7	139.9	13.4	57.5	9.9	650.3	21.5	16.4	5.8
ALCA7-KRA-205	Geologic Alca-7							35227.4	6084	746	393	5648	36.3	163.2	141.4	13.0	57.2	10.6	611.7	21.5	15.7	5.2
Arpu01	Geologic Chivay							37756.5	4755	627	583	5017	41.0	243.5	46.7	18.1	72.5	19.9	184.6	25.7	21.1	9.2

SAMPLE	Group	Type	weight (g)	length (mm)	width (mm)	thickness (mm)	Cortex present/ absent	K	Ca	Ti	Mn	Fe	Zn	Rb	Sr	Y	Zr	Nb	Ba	Pb	Th	U
Arpu02	Geologic Chivay							37268.8	4659	618	563	4960	48.0	245.3	45.6	16.9	71.6	19.2	227.5	23.4	21.8	6.7
Arpu03	Geologic Chivay							35992.8	4733	798	672	5795	42.6	240.2	46.3	16.6	73.0	19.6	198.5	25.1	21.7	7.1
Arpu04	Geologic Chivay							33331.6	4359	745	555	5240	47.4	241.3	46.8	17.0	71.9	18.0	220.7	22.5	19.6	8.2
Arpu05	Geologic Chivay							36494.2	4673	607	593	4907	39.7	242.7	44.5	16.2	70.0	18.3	238.7	23.0	21.2	7.7
Arpu06	Geologic Chivay							37823.0	4722	587	596	5083	41.5	247.2	46.4	16.0	73.7	19.9	178.8	23.8	20.8	8.9
CHV001	Geologic Chivay							34945.6	4085	613	646	5588	41.2	242.5	45.4	17.0	60.0	19.2	176.1	27.8	21.2	7.7
LPP001	Lisahuacho geologic							42318.3	7865	958	339	8732	54.4	160.5	291.3	12.4	159.1	12.8	756.5	26.9	16.9	5.5
LPP002	Lisahuacho geologic							41702.2	7652	969	384	8570	58.6	157.8	285.4	11.8	158.6	12.8	721.0	27.9	17.6	3.8
LPP003	Lisahuacho geologic							41935.6	7721	942	369	8648	55.6	162.0	288.9	12.3	158.2	12.7	606.3	25.5	17.7	3.6
LPP004	Lisahuacho geologic							40862.3	7399	925	374	8414	59.0	156.9	280.7	11.9	156.0	13.2	878.9	27.1	20.0	4.6
LPP005	Lisahuacho geologic							42456.0	7816	948	319	8730	57.9	159.9	291.9	11.8	166.1	13.3	622.6	25.3	16.8	4.4
ANI7151-1-1	Anillo geologic							37200.3	6086	779	340	6057	39.6	174.2	157.8	14.1	112.7	13.3	727.3	21.1	20.0	6.2
ANILLO7151.1.2	Anillo geologic							37104.8	6966	889	451	3224	44.2	173.3	165.6	14.7	115.3	6.5	1068.2	23.0	20.1	4.8
NT0057	Anillo geologic							37733.2	6382	778	388	6166	51.7	178.4	164.7	14.1	111.8	12.6	739.6	20.6	19.9	6.5
NT0062	Anillo geologic							38196.3	6550	775	418	6180	48.3	177.6	164.1	14.1	108.4	12.8	776.9	21.2	20.5	5.6
NT0063	Anillo geologic							39816.5	6675	805	425	6209	45.4	178.1	166.9	13.9	114.2	11.8	745.5	18.9	19.4	7.8
NT0065	Anillo geologic							37874.7	6586	794	333	6450	51.2	179.3	172.3	14.5	113.3	13.2	527.1	20.2	19.5	5.5
PPP001	Potreropampa geologic							38422.5	5153	556	384	4615	39.9	166.7	83.9	14.3	63.1	13.3	361.2	26.7	15.6	6.5
PPP002	Potreropampa geologic							42851.2	5514	587	400	4744	40.8	171.1	83.4	14.0	64.5	13.8	348.8	23.1	15.1	5.4
PPP003	Potreropampa geologic							39887.2	5718	580	372	4789	69.0	173.3	87.2	13.5	63.3	15.1	237.2	21.8	17.4	5.1
PPP004	Potreropampa geologic							44635.4	5387	553	343	4678	40.7	169.0	84.6	13.3	61.8	13.4	249.0	20.9	15.9	5.0
PPP005	Potreropampa geologic							39073.5	5423	562	293	4721	38.8	171.9	83.2	13.1	65.0	14.5	154.6	20.8	16.2	5.3
rlb039	Jampatilla geologic							35366.3	10843	1094	552	8847	70.6	163.3	284.1	25.7	153.6	18.0	666.6	27.1	13.4	6.1
rlb040	Jampatilla geologic							33851.7	10118	983	410	8476	57.0	159.0	273.6	25.3	153.6	17.3	664.6	25.5	12.4	7.2
rlb041	Jampatilla geologic							35258.1	11332	1065	505	8631	57.4	163.1	284.1	25.2	154.3	16.8	614.1	27.9	13.3	5.9
rlb042	Jampatilla geologic							35233.9	11007	1027	378	8927	57.6	161.9	284.5	24.9	152.9	18.3	402.1	27.1	12.8	5.6
rlb043	Jampatilla geologic							34788.5	11289	1062	494	8696	61.2	164.5	281.2	24.9	154.9	17.5	613.9	28.8	12.1	5.5
rlb044	Jampatilla geologic							34217.1	10265	982	464	8614	66.8	160.6	277.9	24.2	149.8	17.2	577.8	25.8	11.5	6.0